MINISTRY OF HIGHER EDUCATION AND

SCIENTIFIC RESEARCH

MOHAMED KHIDER BISKRA UNIVERSITY

Faculty of exact sciences and Natural and life sciences

Department of Material Sciences

THESIS

Presented by

Chennai Hind Yassmine

With a view to obtaining the diploma of:

DOCTORATE IN Chemistry

Option:

Pharmaceutical chemistry

Title:

In silico Investigation of several series of heterocyclic molecules for drug discovery

Defended on:

Before the Examination Commission

Mr.Nadjib MELKEMI	Univ.MohamedKhider-Biskra	President
M.Salah BELAIDI	Univ.MohamedKhider-Biskra	Thesis Director
Mrs.Mebarka OUASSAF	Univ.MohamedKhider-Biskra	Examiner
Mrs.Aicha KERASSA	Univ.-ElOued	Examiner

ACKNOWLEDGMENTS

First and for most, I thank Allah, the Almighty, for presenting me with this chance and bestowing upon me the capacity to succeed. I'd like to thank everyone in my family, no matter how large or tiny. I'd want to express my gratitude to my supervisor, Prof. BELAIDI Salah, whose extensive knowledge and rational manner of thinking have been quite beneficial to me. His understanding, encouragement, and personal mentorship have formed a solid foundation for my thesis. I wish to extend my sincere thanks to Mr. Nadjib Melkemi, Professor at the University of Biskra, for accepting to chair the dissertation of my thesis. I want to give great thanks to the professor MEBARKA OUSSAF Because of the great efforts that she made and helped me in writing my thesis. I would also like to thank the committee member, Sr.KERASSA AICHA, Professors at the University El Oued, for agreeing to examine and judge my work. I'd want to thank everyone in the computational and pharmaceutical chemistry group at Biskra University's LMCE Laboratory for the opportunity to work with them. They offered a nice and cooperative work environment, as well as valuable feedback and insightful remarks on my work.

DEDICATION

This thesis is profoundly dedicated to all.....

My beloved family (my mother, my father, my husband, my bébé Rahaf , my brothers and my all friends).

My hankfulyourendless love, Sypports and Advice.

Table of contents

ACKNOWLEDGMENTS

TABLE OF CONTENTS

LIST OF FIGURES

LIST OF TABLES

LIST OF ABBREVIATIONS

General Introduction…….……. **1**

REFERENCES……**3**

CHAPTER I: The disease of Alzheimer, and the target (acetylcholinesterase)

1.Alzheimer

1.1.Introduction ……..….5

1.2.What is Alzheimer's disease? ……..…6

1.3.Symptoms…….....6

1.4.Stage.....8

1.5.What Causes Alzheimer's ?.....9

1.6.Who gets Alzheimer's disease? ……..……...……....9

1.7.Diagnosis……..……11

1.8.Treatment and support……...…….12

1.9.Medications for congnitive symptoms……...……14

2. Cholinesterase enzyme.....16

2.1. Introduction……...……..……16

2.2. Structural description of Acetylcholinesterase…….....……..16

2.3. Physiological role ..……...……..18

2.4. The active site and the catalytic triad……..…..…….19

2.4.1. The esterase site…….…….20

2.4.2. The anionic site……..……..20

2.5. The peripheral site…….……...…….21

2.6. AChE inhibitors…….…….……..…..……21

2.6.1. According to their origin……..……...…21

2. 6.2. According to their mode of action…….…….…….21

3. Heterocyclic compound…….……25

3.1. Biological Activity of heterocyclic compounds…….…….……..…….26

REFERENCES…….……31

CHAPTER II: Virtual screening

1.Introduction……..…….……..39

2. Virtual in silico screening...……...…….……..….39

2.A. Virtual “ligand-based” screening …… ……..…….…...…...40

2.B. “Structure-based” virtual screening …….....….41

3. Virtual screening tools……...……...…45

3.1. The target…….....…..45

3.2. chemical libraries..... 45

3.2.1. French National Chemical Library…….……...……46

3.2.2. Pubchem…….……..…46

3.2.3.Zinc…….…….…46

3.3. The program.…….……...46

4. Molecular Dynamics ……47

4.1.Dynamic cross-correlation matrices (DCCM.....…….……..47

4.2.Binding free energy calculations…….....……..…...48

4.3.Free energy landscape (FEL)…….....……..49

REFERENCES…….53

CHAPETR III Identification of potent acetylcholinesterase inhibitors as new candidates for Alzheimer disease

1. Introduction……...…….…….....57

2. Materials and Methods……...……59

2.1.Data set……59

2.2.Preparing the Ligand structure…….……60

2.3.Preparing the Protein Structure ……..……60

2.4.Receptor grid generation …….……60

2.5. Development of e-Pharmacophore Hypothesis……..……..61

2.6. Enrichment Calculations…….……61

2.7. Glide Ligand docking……..62

2.8.Structure-based virtual screening…….……63

2.9.In silico ADMET prediction……..63

2.10.Molecular Dynamics Simulation (MDS) ……..……..64

2.11.Dynamic Cross-Correlation Matrix (DCCM) ……...……..65

2.12.Free energy landscape (FEL) ……..66

2.13.Binding Free Energy Calculations…….……..66

3. Discussion…….……...67

4. Results and discussion……...……..69

4.1.Development of e-pharmacophore hypotheses……..69

4.2.Enrichment Calculations……..……...70

4.3.ScreeningE-Pharmacophore-based Virtual Screening…….…..…71

4.4.Glide Ligand docking…….……..……72

4.5.In silico ADMET predictions……...……78

4.6.MD Simulations…….……...82

4.7.Dynamic cross-correlation matrix (DCCM) analysis……86

4.8.Free energy landscape (FEL) ……..……..87

4.9.Binding Free Energy Calculations……...……..89

5.Conclusions ……..……92

REFERENCES…….93

LIST OF FIGURES

CHAPETR I

Figure.1. *Cross section of the brain show atrophy, shrinking or brain tissue caused by alzheir's disease……..…….6*

Figure.2. *The reaction between the neurotransmitter and cholinesterase……..……16*

Figure .3.*Schematic ribbon representation of the 3-D structure of the T.Californica AChE monomer……17*

Figure.4.*Schematic representation of the 3D structure of AchE……18*

Figure .5.*The reaction between AchE and Acetylcholine……19*

Figure.6.*Schematic representation of the mechanism of action of AchE……19*

Figure .7.*The synthesis of miotin from physostigmine……23*

Figure .8. *The new synthesized family of thiazolepiperazine compounds……28*

CHAPETRII

Figure .1.*Conducting a virtual screening experiment via docking ……42*

Figure .2.*Example of Ligand-basd (pharmacophore) and structure-based virtual screening*

steps ……43

Figure.3.*Example of Ligand-basd (E-pharmacophore) and structure-based virtual screening* steps ……44

Figure.4.*The expected FEL for high and low temperatures. The jump motion among the basins becomes slower and slower as the temperature is reduced, and when the mean waiting time for the jump motion exceeds the observation time, the glass transition occurs in the trapmodel……50*

Figure.5.*Contour of the FEL in two principal axes for a model high polymer (Tg = 230 K) determined by MD simulation. While a single basin is seen at 400 K, two basins exist at 200 K. ……51*

CHAPETR III

Figure.1.*(A) Alignment of e-pharmacophore models of Acetylcholinesterase (B) Alignment of e-pharmacophore models of Acetylcholinesterase with the referenceligand(HUP)……69*

Figure .2.*Sketch of the ROC plot used for Validation of e-pharmacophore model……71*

Figur.3.*The reference ligand in the active site of the target Acetylcholinesterase and it's interactions with amino-acid residues……72*

Figure.4.*Superimposition image of the X-ray native pose of co-crystal ligand (HUP) and it's re-docked pose of the co-crystal ligand in the active site of the target PDB-4EY5.Gray color: X-ray native pose,Green color: Re-docked pose……73*

Figure.5.*Interactions between amino-acid residuesand selected molecules(A)CID_44461278,(B) CID_162895946,(C) CID_CID_44285285, (D)CID_81108419,in the active site of the target 4EY5……75*

Figure.6.*Root mean square deviation (RMSD) profiles for backbone atoms of each system……..83*

Figure.7.*Root mean square Fluctuation (RMSF) profiles for backbone atoms of each ……..83*

Figure. 8.*Radius of gyration (Rg) profiles for each system over 100 ns of simulation……85*

Figure.9.*Solvent Accessible Surface Area (SASA) profiles for each system during 100 ns of simulation..86*

Figure. 10.*$C_\alpha$residue cross-correlation computed for the three system, (A) 162895946, (B) 44461278 and (C) HUP……87*

Figure.11.*FEL as a function of RMSD (nm) and radius of gyration (nm) for (α)Acetylcholinesterase_162895946, (β)Acetylcholinesterase_44461278 and (γ)Acetylcholinesterase_HUP.Snapshots of Acetylcholinesterase structures from minimum energy basinswere extracted……89*

Figure.12.*MM-PBSA binding energy decomposition for the three-exanimated systems……91*

Figure S1.*Alignment of respective e-pharmacophore models of 4EY5 with blue color: CID_162895946, gray color: CID_44461278, orange color: CID_44285285, mauve color: CID_81108419……..101*

LIST OF TABLES

CHAPETR I

Table I. *The table includes drugs that have been shown or suspected to produce dementia symptoms.....15*

CHAPETR III

Table.1.*Validation of e-pharmacophore model ……...70*

Table.2 .*Structure, molecular formula, Docking score (SP, XP) kcal/mol, Glide energy and fitness score of selected 4 compounds andreference ligand……...76*

Table.3.*Representations of molecular interactions between CID_ 44461278, CID_162895946, CID_44285285 and CID_81108419ligandsand Acetylcholinesterase receptor……...78*

Table.4.*Estimated physicochemical and pharmacokinetic parameters, Bioavailability Score,Synthetic accessibility properties by QikProp and SwissADME……...81*

Table.5.*Toxicity prediction of the reference compound and selected hits using Protox-II……....82*

Table.6.*ADMET properties of reference compound and selected hits using AdmeLab……..…….....82*

Table.7.*The average values of different parameters obtained through MD simulation……..……..…..86*

Table.8.*The binding free energy in kcal.mol–1 for the three studied systems using MM-PBSA calculations……...91*

LIST OF ABBREVIATIONS

2D: Two dimensions.

3D: Three dimensions.

Å: Angstrom.

ACh: Acetylcholine.

AChE: Acetylcholinesterase.

AD: Alzheimer's disease

AUAC: area under accumulation curve

BEDROC: Boltzmann-enhanced receiver operating characteristic discrimination

BuChE: Butyryl-cholinesterase.

DCCM : Dynamic cross-correlation matrices

DCL: Mild cognitive impairment.

DUD: Decoys database.

EF: the enrichment factor

FDA: Food and Drug Administration

FEL : Free energy landscape

FFMA:T he familial form of Alzheimer's disease.

HA: Huperzine A

IC50: Inhibitory concentration 50.

Kcal: Kilo calories.

KDa: Kilo Dalton.

MD: Molecular dynamics.

MM-PBSA: Molecular Mechanics Poisson-Boltzmann Surface Area

OPLS-3: Optimization Potential Liquid Simulation.

PDB: Protein Data Bank.

PM: Molecular Weight.

Rg: The radius of gyration.

RMSD: Root Mean Square Deviation.

RMSF: The root mean square fluctuations.

ROC: The receiver operating characteristic.

SASA: the solvent accessible surface area.

SP: standard precision.

XP: extra precision.

General Introduction

General Introduction

As the population ages, Alzheimer's disease has emerged as a serious public health issue. It is a neurodegenerative illness of brain tissue that causes gradual and permanent loss of mental function. Alzheimer's disease is the leading cause of dementia in the elderly, affecting an estimated 6.7 million Americans globally [1]. Numerous studies show that the damages induced by Alzheimer's disease mostly impact cholinergic circuits. This causes a significant drop in the quantities of neurotransmitters circulating in the brain. Acetylcholine deficit can approach 90% in extreme cases of the condition and affects the neocortex, hippocampus, Meyert's nucleus basalis, striatum, and thalamus [2]. Doctors typically utilize acetylcholinesterase inhibitors to treat cholinergic insufficiency. These compounds, which block acetylcholine breakdown at the synaptic cleft, have been demonstrated to be useful in treating some Alzheimer's symptoms [3]. We are interested in this approach to therapy via suppression of AChE in the current study. To contribute to the creation of novel AChE inhibitors, we employed in silico virtual screening methods. These approaches include estimating the affinity of à large number of compounds (collected in chemical libraries) for the specified active site, which is simpler to execute and far less expensive than experimental screens. Virtual screening, which began in the early 1980s, has evolved to become a key tool in the hunt for physiologically active drugs, since pharmaceutical companies commit about 10% of their budget on drug-assisted research computer Virtual screening software includes Gold, Glide (Shrodinger) [4], FlexX, and AutoDock Vina [5]. The latter was employed in the current study to propose novel AChE inhibitors via virtual screening, the objective of the present work is, initially, to test the reliability of the pharmacophore model used for the filtration of a database of AChE inhibitors, the validation is relayed by the calculation of the validation parameters such as

thereceiver operating characteristic (ROC) curve, the enrichment factor (EF), area under accumulation curve (AUAC), and BEDROCThe second test consists of visually analyzing the poses of the AChE inhibitors simulated by the software (Schrodinger) by comparing them with those of reference ligands. The method's nameis molecular docking,used to study the interactions and the affinity of ligands for the active site of enzyme [6], the ADMET study performed to study the pharmacokinetics and toxicity of ligands [7], and molecular dynamics used to select the most stable compounds [8].

The manuscript is divided into three chapters:

The primary chapter is a review of the literature that describes the Alzheimer illness (introduction, definition,Symptoms, Who gets Alzheimer's disease?, Diagnosis, Stages,What Causes Alzheimer's ,Treatment and support, Medications for congnitive symptoms), the target (acetylcholinesterase) cibled for the treatment of alzheimer diseases and the various heterocyclic compounds.

The second chapter discusses the several computational approaches used in drug development and studies Structure-based virtual screening and ligand -based virtual screening.

The third chapter involves studies of structure-based virtual screening utilizing e-pharmacophore approaches, molecular docking, ADMET investigation, and molecular dynamics. Identification of potent acetylcholinesterase inhibitors as new candidates for Alzheimer disease via virtual screening, molecular dynamics simulation and MM-PBSA calculations.(Work published in: press in the journal :Molecules ,Vol 11(2), 914-939, 2019: Url de l'article : https://www.mdpi.com/1420-3049/29/6/1232).

Reference

1. Matthews, K. A., Xu, W., Gaglioti, A. H., Holt, J. B., Croft, J. B., Mack, D., & McGuire, L. C. (2018). Racial and ethnic estimates of Alzheimer's disease and related dementias in the United States (2015–2060) in adults aged≥ 65 years. *Alzheimer's & Dementia*. https://doi.org/10.1016/j.jalz.2018.06.3063
2. Mesulam, M-Marsel. "Cholinergic circuitry of the human nucleus basalis and its fate in Alzheimer's disease." Journal of Comparative Neurology 521.18 (2013): 4124-4144. Gustafon,L. Physostigmine ant tetraaminoacridine treatment of Alzheimer's disease. *Acta Neurologica Scandinavica* .1993 ; 88 :149.
3. https://www.schrodinger.com/products/ligprep
4. Arrault A. Stratégies de docking-scoring assistées par analyse de données. Application au criblage virtuel des cibles thérapeutiques COX-2 et PPAR gamma. Thèse de doctorat d'université : Modélisation Moléculaire et Chemoinformatique. Orléans : Université d'Orléans. France. 2007. 176.
5. Molecular Docking—An overview | *ScienceDirect* Topics. (s. d.). Consulté février 2024, à l'adresse https://www.*sciencedirect*.com/topics/neuroscience/molecular-docking
6. Pires, D. E. V., Kaminskas, L. M., & Ascher, D. B.. Prediction and Optimization of Pharmacokinetic and Toxicity Properties of the Ligand. In M. Gore & U. B. Jagtap (Éds.), Computational Drug Discovery and Design (2018) (Vol. 1762, p. 271-284). *Springer New York*. https://doi.org/10.1007/978-1-4939-7756-7_14
7. Processes | Free Full-Text | Molecular Dynamics Simulations in Drug Discovery and Pharmaceutical Development. (s. d.)2024/. https://www.mdpi.com/2227-9717/9/1/71

Chapter I:The disease of Alzheimer and the target (acetylcholinesterase)

1. Alzheimer

1.1 .Introduction

On November 3, 1906, a clinical psychiatrist and neuroanatomist, Alois Alzheimer, presented "A peculiar severe disease process of the cerebral cortex" at the 37th Meeting of South-West German Psychiatrists in Tubingen. He detailed a 50-year-old lady he had been following since her admission for paranoia, progressive sleep and memory problems, violence, and bewilderment, until her death 5 years later. His report identified unique plaques and neurofibrillary tangles in brain histology. It sparked little attention, despite Kraepelin's enthusiastic response, who soon inserted "Alzheimer's disease" in the third edition of his work Psychiatrie in 1910.Alzheimer published three more cases in 1909 and a "plaque-only" variant in 1911, which reexamination of the original specimens in 1993 revealed to be a different stage of the same process. Alzheimer died in 1915, at the age of 51, shortly after assuming the chair of psychiatry in Breslau and long before his name became a household word. Alzheimer's disease was named after Dr. Alois Alzheimer. In 1906, Dr. Alzheimer observed alterations in the brain tissue of a lady who died from an uncommon mental disease. Her symptoms included memory loss, linguistic difficulties, and erratic conduct. After her death, he studied her brain and discovered amyloid plaques and neurofibrillary tangles. Plaques and tangles in the brain remain key hallmarks of Alzheimer's disease [1]. Another hallmark is the loss of neural connections in the brain. Neurons convey signals throughout the brain and to muscles and organs. Researchers are studying the intricate brain changes that cause Alzheimer's disease to develop and advance. Brain injury may begin decades before memory and cognitive issues manifest [2]. During the preclinical stage of Alzheimer's disease, individuals may not exhibit symptoms, yet the brain is undergoing harmful changes [3]. Amyloid plaques and tau tangles are caused by abnormal protein accumulation in the

brain. Healthy neurons die when they cease to function and lose connections with others [4].This factsheet explains Alzheimer's disease symptoms, diagnosis, and risk factors. It also outlines current therapies and support options.

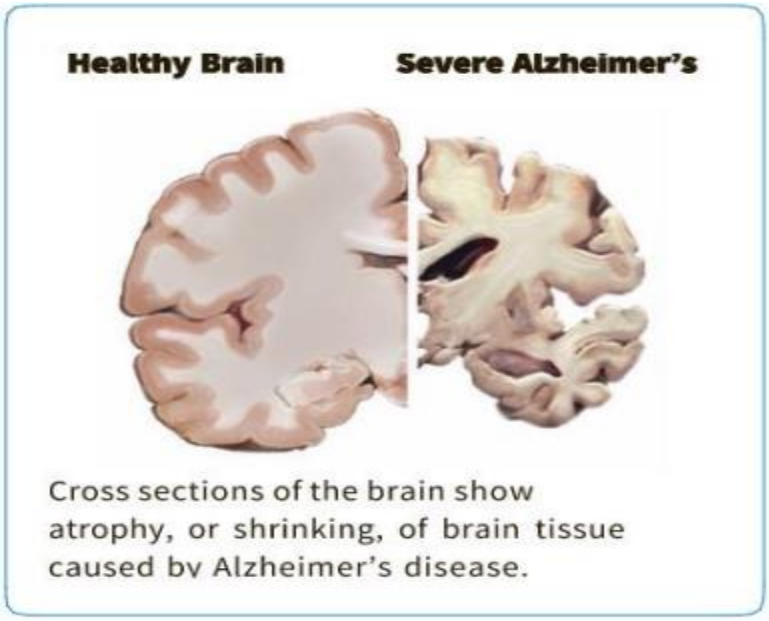

Figure 1.Cross section of the brain show atrophy, shrinking or brain tissue caused by alzheir's disease

1.2 .What is Alzheimer's disease?

Alzheimer's disease is an irreversible, degenerative brain ailment that gradually erodes memory and cognitive abilities, eventually resulting in the inability to perform even the most basic activities[5]. Most persons with Alzheimer's develop symptoms in their mid-60s. Estimates vary, but specialists believe that over 5 million Americans may have Alzheimer's [6].Alzheimer's disease is now the sixth greatest cause of mortality in the US. However, new projections suggest that it may rank third, behind heart disease and cancer, as a cause of death for the elderly [7].

1.3 .Symptoms

Alzheimer's disease is a progressive ailment, which means that the symptoms worsen with time. Memory loss is a major aspect, and it is typically one of the first signs to appear [8].

The symptoms develop gradually over months or years. If they occur over several hours or days, a person may require medical treatment, since this might suggest a stroke.

The symptoms of Alzheimer's disease include:

- Memory failing: A person may have trouble absorbing new knowledge and remembering it. This might result in[9]:
- Repeated queries or conversations.
- Losing things
- forgetting an event or an appointment
- Straying or being lost.
- Memory failing: A person may have trouble absorbing new knowledge and remembering it. This might result in:
- Repeated queries or conversations.
- Losing things
- forgetting an event or an appointment
- Straying or being lost.
- Recognition problems: A person's ability to identify people or things, as well as utilize simple tools, may deteriorate. These disorders are not caused by poor vision.
- Problems with spatial awareness: A person may struggle with their balance, fall over or spill objects more frequently, or have difficulties aligning garments to their body when getting dressed [10].

- Problems with speaking, reading, or writing: A person may have difficulty remembering basic words or make more speech, spelling, or writing errors.
- Personality and behavior changes may include increased agitation, anger, or worry, lack of interest in activities, and less empathy, excessive, obsessive, or socially unacceptable behaviors.

1.4 .Stage

Alzheimer's disease can vary from moderate to severe. The scale progresses from mild impairment to substantial impairment, culminating in severe cognitive deterioration. The parts that follow will go over the various phases of Alzheimer's and some of the symptoms that accompany it [11].

- Mild Alzheimer’s disease

People with mild Alzheimer's disease suffer memory and cognitive issues, which may include the following:

- ✓ Taking longer than usual to complete everyday duties.
- ✓ difficulties managing money or paying debts.
- ✓ Symptoms may include wandering and getting lost, as well as attitude and behavior changes such as increased irritability, concealing items, or pacing.

- Moderate Alzheimer’s disease

Moderate Alzheimer's illness damages the regions of the brain that control language, perceptions, thinking, and awareness. This might result in the following signs.

- ✓ Increased memory loss and confusion
- ✓ Having difficulties identifying friends or relatives
- ✓ An incapacity to learn new things.

- ✓ Difficulty executing multi-stage tasks, such as dressing, and adjusting to new surroundings.
- ✓ Impulsive conduct might lead to hallucinations, delusions, or paranoia.

- ➢ Severe Alzheimer's disease

Plaques and tangles accumulate throughout the brain in severe Alzheimer's disease, causing brain tissue to atrophy significantly. This might lead to:

-Symptoms may include difficulty communicating

-Reliance on others for care

-Difficulty leaving bed for extended periods [12].

1.5 .What Causes Alzheimer’s

Scientists still don't completely grasp what causes Alzheimer's disease in most people. In those with early-onset Alzheimer’s, a genetic mutation is frequently the reason. Late-onset Alzheimer's is caused by a complicated series of brain alterations that occur over several decades. The causes are likely a mix of genetic [13], environmental, and behavioral factors. The significance of any of these variables in increasing or lowering the chance of getting Alzheimer's varies from person to person.

1.6 .Who gets Alzheimer’s disease

Alzheimer's disease is often diagnosed after the age of 65, however it can sometimes affect individuals younger than that age. This is known as early-onset Alzheimer's disease, a kind of young-onset dementia. In the UK, about 40,000 persons fewer than 65 have dementia. Alzheimer's disease is caused by several variables, which are discussed further below. A few of these risk factors (such as lifestyle) may be changed, but others (such as age and genes) cannot [14].

- ➢ **Age**

Age is the most important risk factor for Alzheimer's disease. The condition primarily affects those over 65. Over this age, the chance of having Alzheimer's disease doubles every five years. Dementia affects one in every six adults over the age of 80.

- **Gender**

Alzheimer's disease affects around twice as many women as males over the age of 65, for unknown reasons. This disparity is not entirely explained by the fact that women live longer on average than males. Alzheimer's disease in women may be associated with a deficiency of the hormone oestrogen during menopause.

- **Genetic inheritance**

Several individuals are concerned that the sickness will be handed on to them from a parent or grandmother. Scientists are looking at the genetics of Alzheimer's disease. There are a few families in whom Alzheimer's disease is clearly passed down from generation to generation. In such families, dementia typically develops before the age of 65. However, Alzheimer's illness, which is strongly hereditary, is exceedingly rare.In the great majority of people, genetics have a considerably more mild impact on Alzheimer's disease risk. Several genes have been linked to an increased or decreased risk of acquiring Alzheimer's disease.Individuals who have a close relative (parent or sibling) diagnosed with Alzheimer's after the age of 65 are more likely to get the condition themselves. Living a healthy lifestyle helps lower the chance of Alzheimer's, making it not an unavoidable condition [15].

Individuals with Down syndrome are more likely to acquire Alzheimer's disease due to genetic differences.

- **Health and life style**

Diabetes, stroke, heart issues, high blood pressure, high cholesterol, and obesity in middle age have been linked to an increased risk of Alzheimer's disease and vascular dementia. Anyone can lower their risk by keeping these in check. Early treatment of depression is crucial as it may be a risk factor for dementia [16].Adopting a healthy lifestyle, especially after mid-life, can reduce the risk of developing Alzheimer's disease. To maintain a healthy lifestyle, engage in regular physical activity, maintain a healthy weight, refrain from smoking, consume a well-balanced diet, and limit alcohol use. Maintaining an active lifestyle via physical, social, and mental activities can reduce risk [17].

1.7 .Diagnosis

If you suspect you may have Alzheimer's disease or another type of dementia, consult your GP. Early identification of dementia has several benefits, including explaining symptoms, providing access to treatment, guidance, and support, and allowing for future planning [18].

Alzheimer's disease cannot be diagnosed by a single test. The GP should first rule out other illnesses that may cause similar symptoms, such as infections, vitamin and thyroid deficits (by blood test), depression, and prescription side effects.

The doctor will discuss the patient's medical history and the impact of their symptoms on their daily life with them and a close friend or family member. A general practitioner or practice nurse may request mental ability tests from the patient.

At this point, the GP may believe he or she can diagnose Alzheimer's disease.

If not, they will often send the individual to a specialist. An old-age psychiatrist, typically located at a memory facility, specializes in the mental health of the elderly. A geriatrician, neurologist, or general adult psychiatrist may provide care in a hospital setting.

The professional will examine the individual's symptoms and how they evolved in further depth. Alzheimer's disease often causes progressive memory decline over months. A family member may be more aware of Alzheimer's symptoms than the individual experiencing them [19].

A pen-and-paper exam will measure the person's mental abilities, including remembering and thinking. Individuals with Alzheimer's may have rapid memory loss during testing. Even when asked, they may struggle to retain the information after a few minutes. A brain scan can determine if alterations have occurred. There are several types of brain scans. CT and MRI are the most often utilized imaging techniques. A brain scan can rule out illnesses including stroke, tumor, or fluid buildup in the brain. These can exhibit symptoms similar to those of Alzheimer's. It may also help identify the kind of dementia. A brain scan in early Alzheimer's disease may reveal shrinkage of the hippocampus and surrounding brain tissue.

Communicating the diagnosis clearly to the person and those closest to them is a crucial step for the diagnosis and treatment of Alzheimer's disease, and we should discuss future actions together [20].

1.8. Treatment and support

While there is no cure for Alzheimer's disease, there are several ways to manage the condition and improve quality of life. This will cover drug and non-drug therapy, support, and activities.

Individuals should have the opportunity to discuss their diagnosis with a professional. This might include a psychiatrist, mental health nurse, clinical psychologist, occupational therapist, or general practitioner (GP) [21].

Providing information about available assistance and resources is crucial for maintaining physical and mental health.

Professionals such as GPs, memory service professionals, and local Alzheimer's Society may provide advice on how to best fulfill the requirements of both the individual and their caregivers.

Drug therapies for Alzheimer's disease can temporarily relieve symptoms and delay development in some cases.

Patients with mild to severe Alzheimer's disease or mixed dementia may be administered drugs like donepezil (Aricept), rivastigmine (Exelon), or galantamine (Reminyl). The medicine may increase memory, focus, motivation, and daily activities like cooking, shopping, or hobbies. Individuals with moderate to severe Alzheimer's disease or mixed dementia may be prescribed memantine (Ebixa) [22].

This can improve mental capacities, everyday life, and reduce uncomfortable or problematic behaviors including agitation and delusions. To treat depression or anxiety, cognitive behavioral therapy (CBT) or pharmaceuticals may be used. Counseling may assist the individual in coming to terms with the diagnosis [23].

There are numerous strategies to support independence and cope with memory loss. Practical strategies include creating a regimen and using a pill box on a weekly basis. Assistive technology devices include computerized reminders and calendar clocks.

Alzheimer's patients benefit from engaging in enjoyable activities. Reading and solving puzzles can help people improve their cognitive abilities. Attending cognitive stimulation programs has been shown to benefit one's mental state. Sharing one's life narrative and creating a personal record might improve memory, mood, and overall wellbeing. As dementia progresses, individuals may prefer reminiscing in a broader sense [24].

As time passes, a person's behavior may grow increasingly agitated or aggressive. These behaviors generally indicate a person's distress. This could be due to medical

conditions, miscommunication, frustration, or lack of stimulation. Individualized techniques aim to identify and address underlying causes. Non-drug treatments can also be helpful. Activities such as social interaction, music, reminiscing, and exercise can be significant for individuals. Antipsychotics are typically used as a first-line treatment. These behaviors are likely to distress anyone who cares about the individual with Alzheimer, support for caregivers is especially vital during such times [25].

1.9 .Medications for cognitive symptoms

There are no disease-modifying medications for Alzheimer's disease, although some treatments may alleviate symptoms and enhance quality of life.

Cholinesterase inhibitors are drugs that can help with cognitive symptoms such as memory loss, disorientation, altered brain processes, and poor judgment [26].

They increase neuronal transmission across the brain, which slows the progression of these symptoms. Three commonly used medications approved by the Food and Drug Administration (FDA) to treat Alzheimer's disease symptoms are [27]:

- Aricept (donepezil) treats all stages.
- while Razadyne (galantamine) treats mild-to-moderate stages.
- Rivastigmine (Exelon) is used to treat mild to moderate phases.

Medication that can Mimic Dementia

It is often difficult to separate the different causes of cognitive changes in an elderly person who is taking many medications for medical issues that can all have an impact on mental functioning. If you suspect your drugs are causing memory loss or impairing other cognitive skills, speak with your doctor. They will assist in determining whether medications are interfering with cognitive functioning by carefully re-examining your symptoms' history to understand the most likely causes of the symptoms, reducing or

eliminating specific medications, or replacing necessary medications with alternate drugs with different properties [28].

Table 1. Thetable includes drugs that have been shown or suspected to produce dementia symptoms [29].

Medication Class	Generic Name	Brand Name
Anti-anxiety and Sleeping-Pill Medications (Benzodiazepines)	Lorazepam, Diazepam, Temazepam, Clonazepam	Ativan, Valium, Restoril, Klonopin
Anticholinergics	Benztropine, Tolterodine, Dicyclomine	Cogentin, Detrol, Bentyl
Anticonvulsants	Carbamazepine, Phenobarbital, Phenytoin	Tegretol, Luminal, Dilantin
Antidepressants	Fluoxetine, Sertraline, Citalopram, Escitalopram	Prozac, Zoloft, Celexa, Lexapro
Antihistamines*	Diphenhydramine, Chlorpheniramine, Cetirizine	Benadryl, Chlor-Trimeton, Zyrtec
Antiparkinson Drugs	Levodopa, Amantadine, Tolcapone	Dopar, Symmetrel, Tasmar
Cardiovascular Drugs	Warfarin, Atenolol, Metoprolol	Coumadin, Tenormin, Lopressor
Chemotherapeutic Agents	Busulfan, Cytarabine	Busulfex, Depocyt
Corticosteroids	Prednisone, Cortisone Acetate, Methylprednisolone	Deltasone, Cortone, Medrol
Narcotics	Oxycodone, Morphine, Codeine (and acetaminophen)	Oxycontin, Roxanol, Tylenol with Codeine

Non-benzodiazepine Sedatives	Pentobarbital, Mephobarbital	Nembutal, Mebaral
Statins	Atorvastatin, Simvastatin, Rosuvastatin	Lipitor, Zocor, Crestor

2. Cholinesterase enzyme

2.1. Introduction

Cholinesterase is a group of enzymes that catalyze the hydrolysis of the neurotransmitter acetylcholine (ACh) into choline and acetic acid (**figure 2**) [17].

Figure.2. The reaction between the neurotransmitter and cholinesterase.

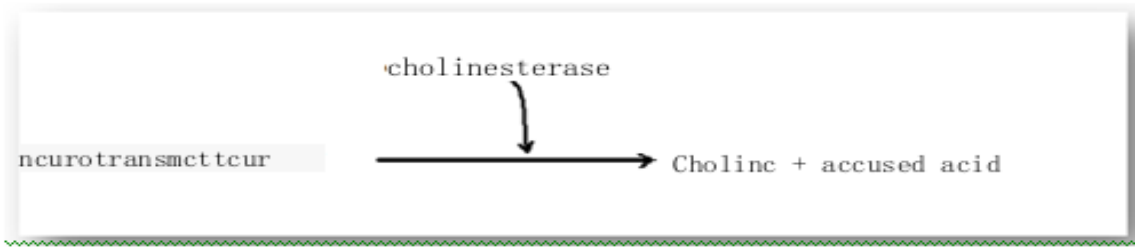

It is a crucial response that allows a cholinergic neuron to return to its resting state following activation.

This family of enzymes has two major classes:

- Pseudo-cholinesterase (BuChE):

Also known as plasma cholinesterase, butyryl-cholinesterase, or acylcholine acylhydrolase, is predominantly present in the liver. BuChE, unlike acetylcholinesterase, hydrolyzes butyrylcholine at à faster rate[18].

- Acetylcholinesterase (AChE):

Is present in a variety of tissues, including nerves, muscles, central and peripheral tissues, motor and sensory fibers, and cholinergic fibers [18].

2.2. Structural description of Acetylcholinesterase

Acetylcholinesterase is a serine protease, comprising 537 amino acids (75 kDa), expressed in the nervous and blood systems of higher eukaryotes. Its physiological role in the circulatory system remains to be elucidated, unlike that of the nervous system, which is perfectly characterized. It is found in particular at the level of so-called cholinergic synapses using the neurotransmitter acetylcholine (ACh). Such synapses are found at neuromuscular junctions as well as in areas of the cortex responsible for cognitive functions (memory, orientation, judgment, etc.) [19].

AChE was first identified in 1867 from the torpedo poison (Torpedo californica). X-ray crystallography reveals valuable information about its three-dimensional structure. Indeed, this enzyme must be in dimeric form to act as a serine protease. Each subunit contains 11 standard β-sheets surrounded by 15α-helices, as well as a short portion of sheet at the Nterminal end, which is not engaged in any interaction with the rest of the structure. Likewise, the presence of three short standard β sheets that are not connected by hydrogen bridges at the heart of the enzyme is noted (**figure 3**) [19].

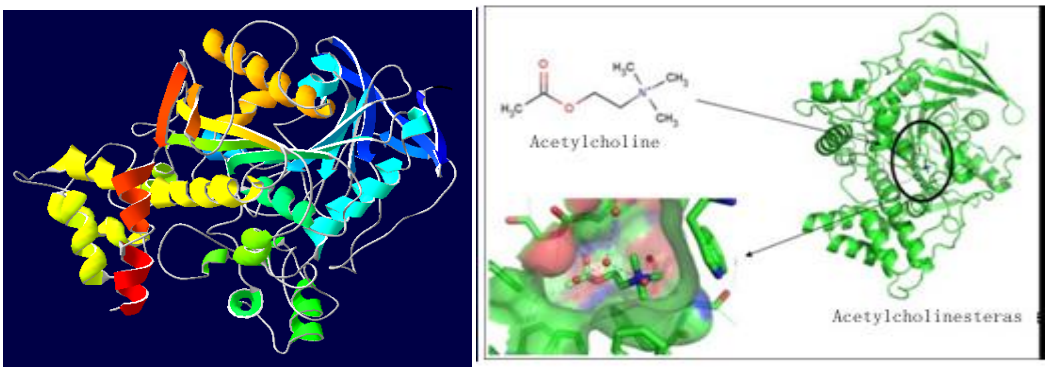

Figure 3: Schematic ribbon representation of the 3-D structure of the T.Californica AChE monomer.

The enzyme's overall folding is typical of the hydrolase family. In the dimer, the two monomers are bound together by a "4-helix bundle": two helices from each monomer, including the C-terminal helix, contribute to the formation of an extremely stable inter-residue linkage. The C terminal cysteines (Cys537) of the two monomers form an inter-

chain disulfide bridge, stabilizing the enzyme's quaternary structure. In an AChE monomer, we identify two domains that are independent of one another and located on either side of the groove leading to the active site. These domains correspond to the two halves of the polypeptide chain: the domain consisting of residues 1–305 adjoins the other, consisting of residues 306 to 537 [19].

A closer look at AChE's 3D structure reveals two critical zones for enzymatic catalysis: the peripheral site at the throat's entry and the active site at the bottom, which houses the catalytic machinery. The active and peripheral sites will thus be two possible targets for AChE inhibition by therapeutic drugs (**Figure 4**).

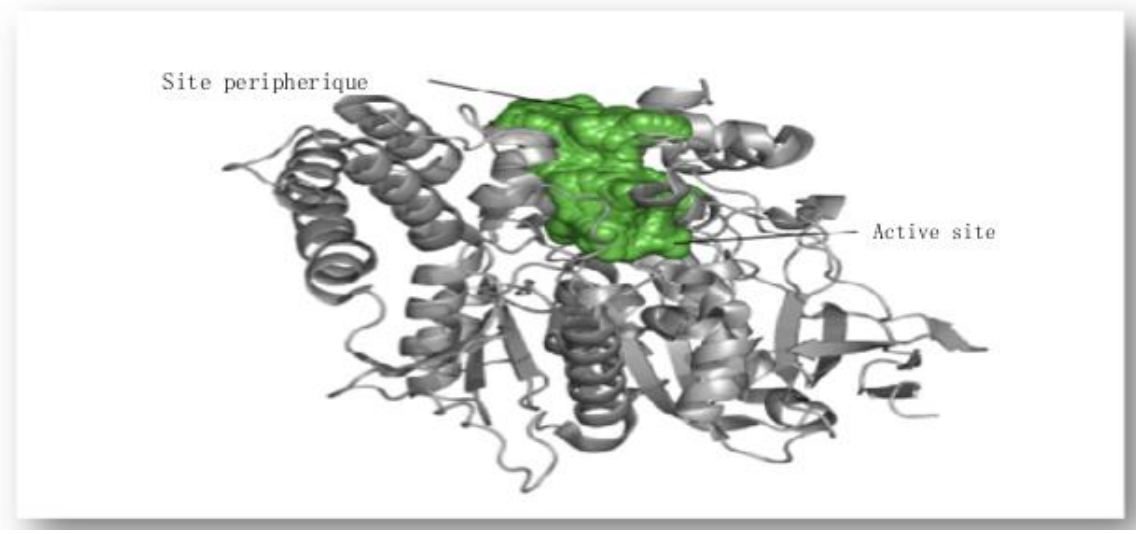

Figure 4: Schematic representation of the 3D structure of AChE.

2.3. Physiological role

Acetylcholine is one of the neurotransmitters most closely associated with storing memories, consolidation, and recall. It is an essential chemical messenger that neurons utilize to deliver messages that support both cognitive processing and basic thinking. Optimal acetylcholine levels may contribute to improved ability to work or short-term memory, increased fluid intelligence, reasoning and logical thinking skills, creative thinking, executive function, attention control, and more vivid nighttime dreams. To minimize neuronal overexcitation, the ACh must be broken down as soon as feasible after signal transmission. This is where the AChE comes in.

The primary physiological function of this enzyme is to regulate cholinergic excitation in the brain by rapidly breaking down excess acetylcholine. It is crucial to note that AChE is one of the quickest enzymes known, with a "turnover" of 1000 to 20,000 molecules per second depending on the species studied. Several studies, however, have found decreased acetylcholine levels in Alzheimer's disease patients. Inhibiting AChE improves ACh levels and alleviates symptoms associated with Alzheimer's disease (**Figure 5**) [20].

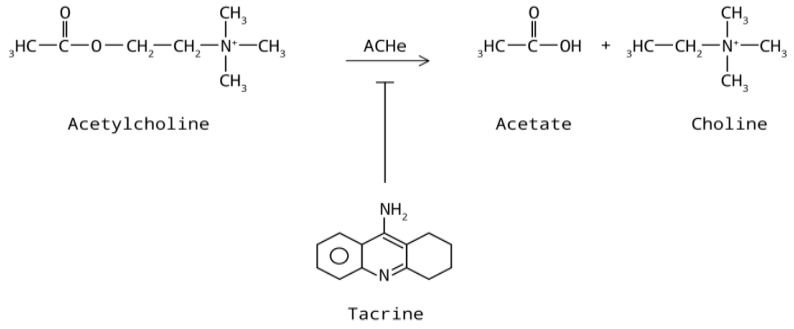

Figure .5.The reaction between AchE and Acetylcholine.

The mechanism of action of acetylcholine esterase is similar to that of chymotrypsin. A nucleophilic serine residue combines with acetylcholine, which contains an ester group, resulting in an intermediate "acetyl-enzyme" complex. As a result, ACh will be cleaved to release choline in the first place. What remains is the acetyl-enzyme complex, which will be hydrolyzed in a subsequent stage to yield acetic acid. The products of this reaction are taken back to the presynaptic terminal, where they are reformed into acetylcholine, which is subsequently employed to convey further signals (**figure 6**) [19].

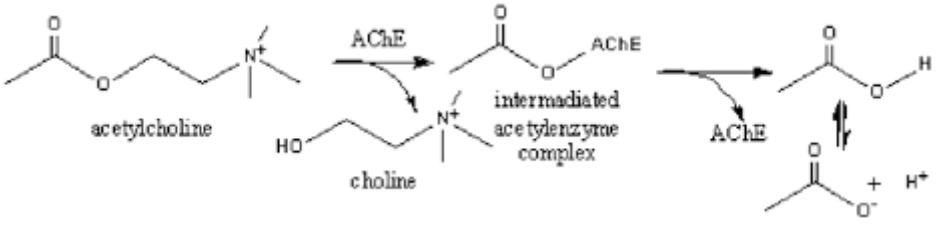

Figure .6.Schematic representation of the mechanism of action of AChE.

2.4. The active site and the catalytic triad

AChE is a dimeric enzyme with 537 amino acids. Structurally, its active region contains a few particular amino acids that play an important role in the stability of the AChE-ACh complex. A 1991 research by J. Sussman et al. identified the active site of AChE as the amino acids Glu 327, His440, and Ser200, located at the base of a 20 Å groove. At this level, we discriminate between two sites: anionic and esterase.

2.4.1. The esterase site

corresponds to the binding site for the acetyl component of the ACh molecule. The ACh is subsequently cleaved, releasing both choline and the "enzyme-acylated" intermediate. Then deacetylation occurs, regenerating the free enzyme and acetate. The catalytic triad consists of residues Ser200, Glu327, and His440. The carbonyl component of the ACh molecule is linked at the catalytic serine (200).His440, for its part, acts as an acid-base catalyst, forming and decomposing the "acetyl-enzyme" intermediate. Its imidazole nucleus forms two hydrogen bonds with Ser200 and Glu327, which serve as the last proton donor and acceptor in this catalytic triad, respectively. The enzyme must be capable of stabilizing ACh's carbonyl oxygen, which becomes negatively charged during the development of the "acetyl-enzyme" intermediate. Similarly, we see the presence of a tiny hydrophobic cavity known as the "acyl pocket" near the esterase site, which is composed of residues Trp233, Phe288, Phe290, and Phe331. This pocket is critical to the stability of the substrate's hydrophobic segment [21].

2.4.2. The anionic site

Gets its name from history rather than its own reality. Indeed, because ACh has a positive charge, it was proposed that the active site of AChE may be made up of a cluster of acidic residues (negatively charged at physiological pH), which would have been responsible for stabilizing the substrate during catalysis. In actuality, the place

where the substrate's tetramethylammonium portion (TMA) will be stabilized is aromatic rather than anionic, consisting of Trp84, Glu199, and Phe330. The electrostatic attraction of the Glu199 residue efficiently stabilizes the ligand's positive charge, but its interaction with the electrons of the surrounding aromatic nucleus is even more powerful.This anionic subsite is critical for catalysis, accounting for more than half of the substrate's stabilizing energy. The residues Trp84 and Phe330 will contribute the most to this stabilizing energy [17].

2.5. The peripheral site

Residues Trp 279 and Tyr 70, as well as the two amino acid series (270-278 and 251-266), make up the peripheral site (PAS: peripheral anionic site), which is positioned at the periphery of the enzyme's cavity (throat). The ligand's interaction at the peripheral location permits the substrate to enter the groove (by steric hindrance). This location will thus be a possible target for AChE inhibition [18].

2.6. AChE inhibitors

Acetylcholine levels normally fall with age, resulting in reduced brain plasticity and learning problems. Indeed, cholinergic neurons are known to perish at a faster rate. Acetylcholinesterase inhibitors have been demonstrated to be quite successful in improving memory capacity in these individuals by naturally compensating for decreased cholinergic activity. Currently, a large variety of AChE inhibitors have been found and may be categorized based on their origin and/or inhibition mechanism [19].

2.6.1. According to their origin

- **Natural origin**

Pharmaceutical firms are increasingly focusing on extracting, purifying, and identifying compounds from natural matrices that can inhibit AChE with little, if any, negative

effects. Currently, various families of natural compounds are recognized for their inhibitory action on this enzyme, including alkaloids and flavonoids [20].

- **Alkaloids**

These are natural organic compounds, most of which are plant-based, more or less basic nitrogenous, have a limited distribution, and have significant pharmacological activities at low concentrations. Currently, numerous alkaloids are thought to inhibit AChE [21].

A. Galantamine

Galantamine, a tertiary alkaloid, is a selective, competitive, and reversible inhibitor of acetylcholinesterase. This chemical, which was initially isolated from the flowers of Galanthus Caucasius, is licensed for the treatment of Alzheimer's disease under the name (Reminyl®). Several compounds were shown to have a stronger inhibitory effect than galantamine [22].

B. Physostigmine

Also known as eserine, this alkaloid has an IC50 of 0.15 uM and has the ability to inhibit AChE. It was initially discovered in 1864 as the active element in the Calabar bean, physostigma venenosum. The usage of physostigmine has been found to enhance memory and cognitive abilities in Alzheimer's patients. However, the molecule's interest is restricted due to its short half-life [23].

C. Huperzine A

It's another alkaloid that inhibits AChE. This chemical, isolated from the Chinese medicinal plant Huperzia serrata, has a strong inhibitory impact while being extremely low in toxicity. It was used as the starting chemical in the development of numerous derivatives [24].

- **Flavonoids**

Flavonoids are the most abundant polyphenolic chemicals generated from higher plants. They are well-known for their antiviral, anti-radical, anti-allergic, anti-tumor, anti-inflammatory, and anticancer properties. Certain flavonoids, particularly flavonols, are known to inhibit AChE. With this in mind, a 2007 research by Jung M et al. found that the ethyl acetate phase of an extract from the Agrimonia pilosa plant is efficient in lowering the biological activity of the enzyme under consideration. A further in-depth investigation along the same lines demonstrated that quercetin, tiliroside, 3-methoxy quercetin, and quercitrin are AChE inhibitors [25].

- **semi synthetic**
  - **Miotin**

It is a semi-synthesised inhibitor derived from physostigmine (**Figure 7**). Miotin, the first carbamate inhibitor, was licensed by the European Agency for the Evaluation of Medicines in 1998 and the Food and Drug Administration in 2000 [26].

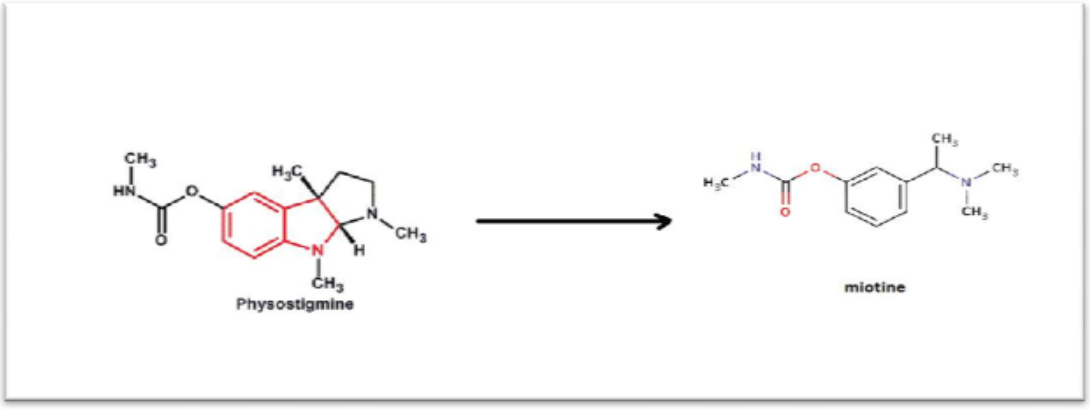

Figure 7. The synthesis of miotin from physostigmine.

- **Synthetic inhibitor**
  - **Donepezil**

Donepezil, also known as donepezil hydrochloride, was approved by the FDA in 1996 and is the second AChE inhibitor marketed under the brand name Aricept®. According to a research published in The New England Journal of Medicine, donepezil, a standard

medication for the early stages of Alzheimer's disease, is also effective in more severe cases [27].

- **Rivastigmine**

Rivastigmine is an irreversible AChE inhibitor. This chemical, marketed as Exelon®, operates on both AChE and BuChE by producing a complex connected by a covalent connection, resulting in the enzymes' transitory deactivation. In healthy young people, a dosage of 3 mg orally reduces acetylcholinesterase (AChE) activity in the CSF by roughly 40% within an hour and a half after administration. Enzymatic activity recovers to its baseline level around 9 hours following the peak of inhibitory activity [28].

- **Tacrine**

Tacrine is a chemical that has been utilized to treat memory impairments in Alzheimer's disease patients, allowing for the first time to achieve some degree of improvement. Tacrine, the first AChE inhibitor accessible, has been sold in the United States since 1993 and in France since 1994 under the brand name (Cognex®). This medicine may produce adverse symptoms associated with excess acetylcholine, such as nausea, vomiting, diarrhea, stomach cramps, and excessive salivation. It also appears that ingesting extremely high dosages of tacrine is harmful to liver cells [29].

2.6.2 According to their mode of action

AChE inhibitors are classified into three types based on their method of action: irreversible, pseudo-irreversible, and reversible.

- **Irreversible inhibitors**

Organophosphates are chemicals that permanently inhibit AChE. Metrifonate, a member of this category, has modest inhibitory effect on the enzyme. This chemical was pulled from the market due to negative effects such as muscular weakness and respiratory issues [30].

❖ **Pseudo-irreversible inhibitors**

This family of inhibitors comprises substances containing a carbamate functional group. The AChE triad catalyzes the carbamylation process. These complexes containing Ser200 hydrolyze at a slower pace than the ACh-AChE complex. The first inhibitor of this type explored for the therapy of Alzheimer's disease was physostigmine, but it was rejected due to its short half-life. Several analogues were investigated to demonstrate its potential. Rivastigmine, a derivative of miotin, is another pseudo-irreversible inhibitor with a carbamate group [23].

❖ **Reversible inhibitors**

These compounds can inhibit AChE by forming weak bonds such as hydrogen, hydrophobic contacts, Van der Waals, and so on. We distinguish:

A. Aminoacridines

Tacrine (Cognex), approved by the FDA in 1993, was the first AChE inhibitor to enter the market. Tacrine, with an IC50 of 8.2 nM, is one of the most effective AChE inhibitors. Subsequently, the basic structure of tacrine was utilized to synthesize additional compounds with similar inhibitory action but less side effects, such as Valnacrine and Suronacrine [31].

B. N-Benzylpiperidines

Donepezil is the second AChE inhibitor authorized by the FDA. It has a higher selectivity for AChE than BuChE. TAK-147 is likewise part of this family of compounds. Although this molecule's inhibitory efficacy is lesser than that of Donepezil, clinical studies are now being conducted [32].

C. Alkaloids

Alkaloids, such as galantamine (reminyl), huperzine, and physostigmine, are also thought to be reversible AChE inhibitors.

3. Heterocyclic compounds

Heterocyclic compounds are cyclic organic substances with at least one heteroatom (not carbon) in the ring structure. The most prevalent heteroatoms include nitrogen (N), oxygen (O), and sulfur (S) [1]. Heterocyclic compounds are often found in plants and animals, accounting for about half of all organic compounds. Natural heterocyclic compounds include alkaloids, colors, medicines, proteins, and enzymes. Heterocyclic compounds are easily categorized depending on their electrical structure.Heterocyclic compounds are often classed as saturated or unsaturated. Saturated heterocyclic compounds exhibit changed steric characteristics, similar to acyclic derivatives. This group includes typical amines and ethers, such as piperidine and tetrehydrofuran. Unsaturated heterocyclic compounds with 5- and 6-member rings have been widely researched due to their unstrained nature [2]. Unstrained unsaturated heterocyclic compounds include pyridine, thiophene, pyrrole, furan, and their benzo fused derivatives [3].Some notable examples of benzo fused heterocycles are quinoline, isoquinoline, indole, benzothiophene, and benzofuran. Heterocyclic compounds are widely used in medicines, agrochemicals, and veterinary goods [4]. Many heterocyclic chemicals are extremely beneficial and necessary for human survival. Heterocyclic compounds include hormones, alkaloids, antibiotics, vital amino acids, hemoglobin, vitamins, dyes, and pigments.

3.1.Biological Activity of heterocyclic compounds

Cyclic compounds have several therapeutic benefits, Among these benefits are the following:

- Anti-fungal properties

Fungal infections most commonly affect the skin, hair, and nails. These chemicals or

medications are employed to treat certain ailments. Ringworm and athlete's foot are examples of prevalent fungal infections. Antifungal drugs kill fungus directly or indirectly by affecting the substances in the cell membrane. According to Al-Mulla et al. [10], some derivatives of dipicolinic acid can be employed as antifungals.

Chitra et al. (2017) synthesized chalcone derivatives as heterocyclic compounds with five-membered rings and used them for antifungal action [11].

- Anti-inflammatory

Anti-inflammatory properties refer to a chemical or treatment's ability to decrease inflammation. Unlike opioids, which target the central nervous system, most analgesics reduce inflammation to relieve pain. Achar et al [12] synthesized 2methylaminobenzimidazoles and investigated their analgesic and anti inflammatory effects in vivo. The synthesised compounds had strong analgesic and anti-inflammatory benefits compared to the reference medication nimesulide.

El-Hashash et al. (2015) [13] synthesized spiro heterocycles and heterocyclic chalcone derivatives and tested them for antibacterial activity. Against all of the pathogens tested, the majority of the synthesized compounds displayed the highest antibacterial activity.

- Activity of antioxidants

The chemical process known as oxidation has the ability to generate free radicals and initiate a chain reaction that destroys cells. Typically, the phrase "antioxidant" refers to two types of drugs: those added to prevent oxidation and natural substances found in meals and human tissue that are thought to have positive health benefits. Thiols and ascorbic acid are examples of chemicals that block other molecules' oxidation processes, allowing them to break the chain reaction and avoid cell harm. Sauer et al. (2017) [14] developed novel compounds with heterocyclic organosulfur on one side and

organoselenium on the other, resulting in antioxidant activity. In both ways, the compounds have significant antioxidant properties.

- Anticancer Activity

Cancer is a disease caused by excessive cell proliferation that can spread throughout the body. This sickness can be caused by exposure to radiation and other chemicals. Pharmaceuticals have been produced to cure diseases by decreasing cancer cells or preventing their proliferation.

Liu et al. (2017) [15] developed new phenanthroindolizidine and phenanthroquinolizidine compounds for anticancer applications.

- **Alzheimer's Disease Prevention**

Alzheimer's, which is the most common degenerative brain illness, is characterized by cognitive impairment. Alzheimer's patients struggle to remember new information, making living challenging. This sector produces new pharmaceuticals at a rapid pace.

Osmaniye et al. [16] developed a new class of thiazolepiperazine chemicals (**Figure 8**). All of the generated compounds strongly inhibited the acetylcholinesterase (AChE) enzyme. However, no treatment significantly lowered the activity of the enzyme butyrylcholinesterase (BChE).

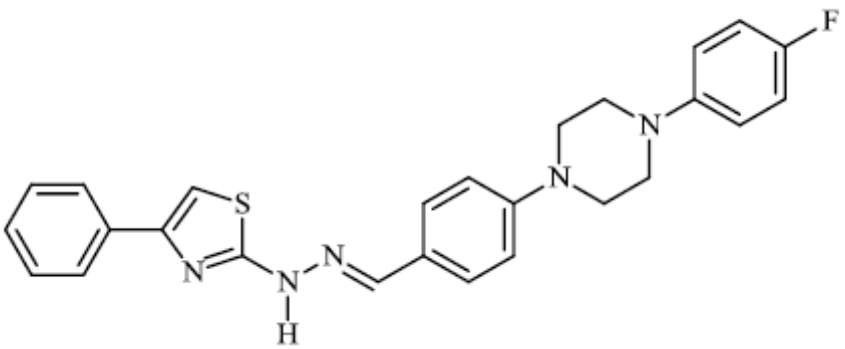

Figure 8. The new synthesized family of thiazolepiperazine compounds.

Refrence:

1. Maurer, K., Volk, S., & Gerbaldo, H.. Auguste D and Alzheimer's disease. *The lancet*, 1997, vol. 349, no 9064, p. 1546-1549.
2. Lovestone S. Fleshing out the amyloid cascade hypothesis: the molecular biology of Alzheimer's disease. *Dialogues Clin Neurosci*. 2000;2:101-110.
3. Alzheimer A. Die diagnostischen Schwierigkeiten in der Psychiatrie. Z Ges Neurol Psychiatr. 1910:1:1-19.
4. Schachter AS, Davis KL. Alzheimer's disease. *Dialogues Clin Neurosci*. 2000;2:91-100
5. J. LCummings.,G. Cole. Alzheimer disease, *Journal of the American Medical Association.* 2002; 287 : 23.
6. JJ Hauw., B. Dubois. M.Verny. CH. Duychkaerts. La maladie d'Alzheimer. *Pathologie. Science*. 199; 162 : 162.
7. Gustafon., L .Physostigmine ant tetra amino acridine treatment of Alzheimer's disease. *Acta Neurologica Scandinavica* .1993 ; 88 :149.
8. Arrault A. Docking-scoring strategies assisted by data analysis. Application to virtual screening of COX-2 and PPAR gamma therapeutic targets. University doctoral thesis: Molecular Modeling and Chemoinformatics. Orléans: University of Orléans. France. 2007. 176.
9. Molecular mechanisms in neurodegenerative dementias. Alzheimer's disease: lesional and molecular diagnostic and therapeutic aspects. http://www.mmdn.univ-montp2.fr/08/04/2015.
10. Alzheimer's disease international. World Alzheimer Report . https://www.alz. co.uk/. 12/05/2015.
11. Djazairess. Alzheimer's disease under debate. http://www.djazairess.com/fr/lqo/51667.17/04/2015.
12. Couderc.A. the search for biological markers of Alzheimer's disease. Annals of Clinical Biology. 2000; 58:40.

13. Lebert, F. ; Pasquier, F. Behavioral and psychological signs and symptoms of dementia. Medical-surgical encyclopedia.1999; 35:7.
14. Alzheimer Society Canada. Alzheimer's disease and risk factors. http://www.alzheimer.ca/fr.08/04/2015.
15. Laurent Letrilliart., Denis Pouchain. Therapeutic management of Alzheimer's disease and related dementias. Exercise- The French journal of general medicine.2011;22:9.
16. Scheltens, P., De Strooper, B., Kivipelto, M., Holstege, H., Chételat, G., Teunissen, C. E., ...& van der Flier, W. M. (2021). Alzheimer's disease. *The Lancet*, *397*(10284), 1577-1590.
17. Scheltens, P., Blennow, K., Breteler, M. M., De Strooper, B., Frisoni, G. B., Salloway, S., & Van der Flier, W. M. (2016). Alzheimer's disease. *The Lancet*, *388*(10043), 505-517.
18. Ballard, C., Gauthier, S., Corbett, A., Brayne, C., Aarsland, D., & Jones, E. (2011). Alzheimer's disease. *the Lancet*, *377*(9770), 1019-1031.
19. Blennow, K., de Leon, M. J., & Zetterberg, H. (2006). Alzheimer's disease. *The Lancet*, *368*(9533), 387-403.
20. Masters, C. L., Bateman, R., Blennow, K., Rowe, C. C., Sperling, R. A., & Cummings, J. L. (2015). Alzheimer's disease. *Nature reviews disease primers*, *1*(1), 1-18.
21. Cummings, J. L. (2004). Alzheimer's disease. *New England journal of medicine*, *351*(1), 56-67.
22. Querfurth, H. W., & LaFerla, F. M. (2010). Alzheimer's disease. *New England Journal of Medicine*, *362*(4), 329-344.
23. Bush, A. I. (2003). The metallobiology of Alzheimer's disease. *Trends in neurosciences*, *26*(4), 207-214.
24. Nussbaum, R. L., & Ellis, C. E. (2003). Alzheimer's disease and Parkinson's disease. *New england journal of medicine*, *348*(14), 1356-1364.

25. *Alzheimer's disease: Symptoms, stages, causes, and treatments*. https://www.medicalnewstoday.com/articles/159442#what-is-it (accessed 2024-02-04).
26. Hippius, H.; Neundörfer, G. The Discovery of Alzheimer's Disease. *Dialogues Clin Neurosci***2003**, *5* (1), 101–108.
27. Rezai, A. R., D'Haese, P. F., Finomore, V., Carpenter, J., Ranjan, M., Wilhelmsen, K., ...& Haut, M. W. (2024). Ultrasound Blood–Brain Barrier Opening and Aducanumab in Alzheimer's Disease. *New England Journal of Medicine*, *390*(1), 55-62.
28. Jung, Y., & Damoiseaux, J. S. (2024). The potential of blood neurofilament light as a marker of neurodegeneration for Alzheimer's disease. *Brain*, *147*(1), 12-25.
29. Wang, H. S., Karnik, S. J., Margetts, T. J., Plotkin, L. I., Movila, A., Fehrenbacher, J. C., ... & Oblak, A. L. (2024). Mind Gaps and Bone Snaps: Exploring the Connection Between Alzheimer's Disease and Osteoporosis. *Current Osteoporosis Reports*, 1-12.
30. Biologie Médicale spécialisée. Cholinestérase. http://www.biomnis.com 20/04/2015.
31. Mirjana B., Colovi.Z Danijela. Krsti.D Tamara. Lazarevi. M Aleksandra. Vesna M Vasi. Acetylcholinesterase Inhibitors: Pharmacology and Toxicology.Current Neuropharmacology .2013;11:21.
32. Jacques-Philippe Colletier. Study of structure-dynamic-function relationships within acetylcholinesterase. University doctoral thesis: Biomolecules. Grenoble: Joseph-Fourier University. France.2006.273.

Chapter II: Virtual screening

1. Introduction

The development of new pharmaceuticals is a long and tedious process that takes ten or even fifteen years and costs roughly a billion dollars. The traditional method for developing a new drug was based on high throughput screening (HTS), in which a large number of compounds are tested in vitro on a given therapeutic target (enzyme, receptor, etc.) to identify hits ("hits" or even promoter compounds), which are then optimized and tested in vivo. However, high-throughput screening immediately encountered significant scientific, technological, methodological, budgetary, and organizational challenges. If we test a vast number of compounds on a certain target, we will surely discover a molecule that is active and stable on that target, but when and at what cost? To answer these two problems, new techniques such as virtual screening by molecular docking, E-pharmacophore and moleular dynamics were required [1].

2. In silico virtual screening

The discovery of bioactive molecules is an expensive and time-consuming process and new strategies are continuously searched for in order to optimize this process. Virtual Screening (VS) is one of the recent strategies that has been explored for the identification of candidate bioactive molecules. The number of new techniques and software that can be applied in this strategy has grown considerably in recent years, so, before their use, it is necessary to understand the basics an also the limitations behind each one to get the most out of them. It is also necessary to assess the real contributions of this strategy so that more significant progress can be made in the future. In this context, this review aims to discuss some important points related to VS, including the use of virtual ligand and biotarget libraries, structure based and

ligand-based VS techniques, as well as to present recent cases where this strategy was successfully applied.

In silico virtual screening is a novel technique for creating new medications that involves estimating the affinity of a large number of molecules (collected in chemical libraries) for the specific active site in order to narrow down the list of molecules with the required activity. These compounds will be investigated experimentally to confirm the hypothesis. This strategy has been successful in bringing a number of medications to market, including ***indinavir (DB00224)***, a powerful HIV protease inhibitor, and ***celecoxib (DB00230),***which specifically inhibits cyclooxygenase 2. [2].Depending on the nature of the experimental information available, there are two approaches for virtual screening. The first, based on the knowledge of a sufficient amount of information concerning one or more active reference molecules, is called "ligand-based virtual screening". The second, based on the structure of the target, is known as “structure-based virtual screening”. Although these two approaches are mainly used exclusively (often because the nature of the initial data leaves only one possible choice), their combination during a screening campaign makes it possible to maximize the chances of success in identifying new keys.

2.A. Virtual “ligand-based” screening

A pharmacophore is a collection of characteristics that a molecule must possess in order to be active. A pharmacophoric model is a spatial arrangement of points created by aligning chemicals with known or inferred modes of receptor interaction. Each point in this model represents 3D coordinates, a volume (usually spherical), and physicochemical attributes (lipophilicity, hydrogen bond donor/acceptor). Its development begins with the selection of active molecules for the desired target. Conformations are then produced, and a hypothetical one is chosen. After aligning the

selected poses, the important locations responsible for the receptor affinity may be deduced.

The advantage of combining this approach with docking is that it allows for the immediate elimination of undesirable molecules, saving calculating time. Furthermore, such a technique allows us to guide the incremental synthesis of the ligand inside the active site. [3]

2.B. “Structure-based” virtual screening

For its part, the "structure-based" approach frequently refers to protein-ligand docking methods. These approaches include evaluating the structural complementarity of each screened molecule while taking the active site into account. This technique, unlike the one based on reference ligands, has the potential to find novel classes of active compounds. On the other hand, these methodologys are often more expensive in terms of processing power, and their use frequently necessitates more experience [3].

- **Molecular Docking :**

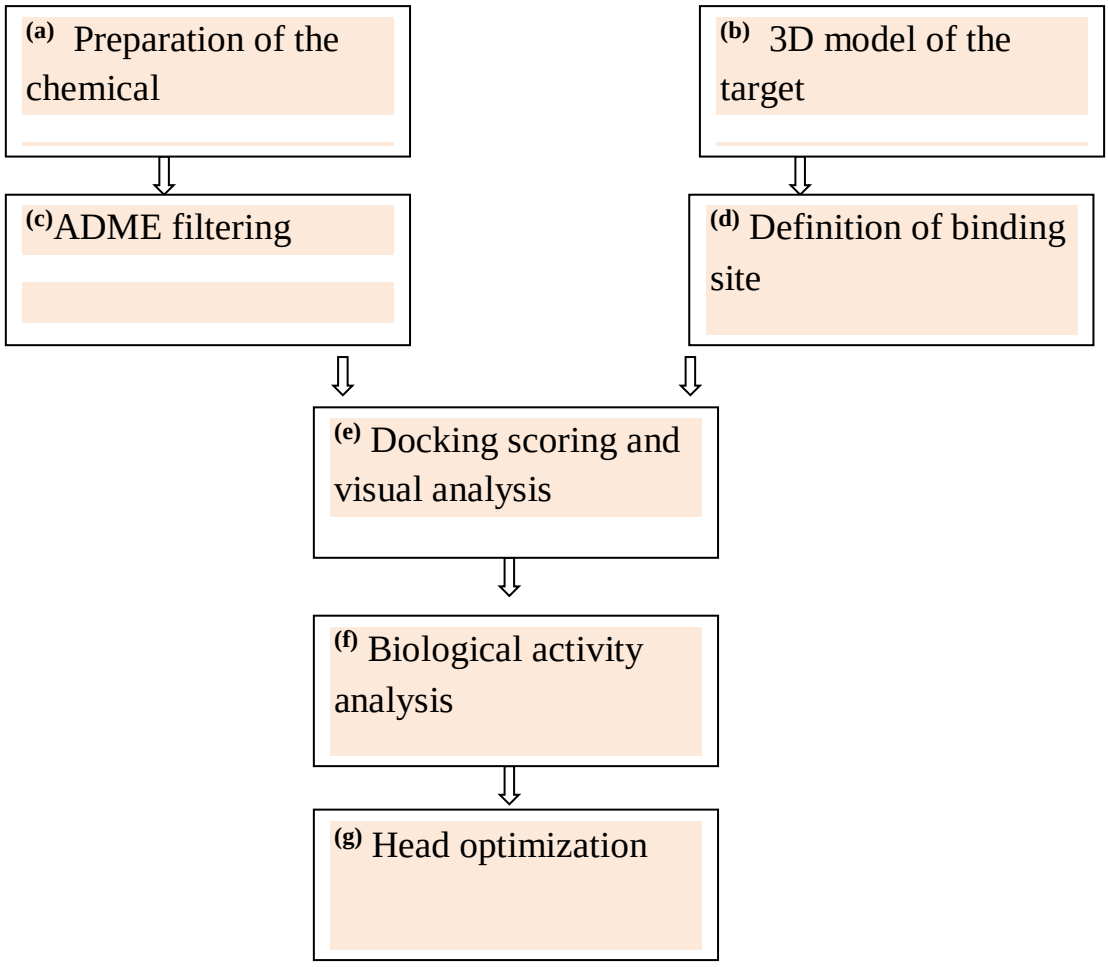

Figure 1. Conducting a virtual screening experiment via molecular docking

First, the chemical library to be screened is prepared (a), followed by pre-filtration (c). Concerning the target, it is important to have a trustworthy three-dimensional structure of the targeted protein (particularly at its active site) (b), which can be obtained using experimental techniques such as X-ray diffraction or NMR, or via a verified homology model. Once the target has been chosen and prepared, its active site is characterized, which consists of defining the essential residues of the binding site that form the molecular recognition locus with the reference ligands (d).When the small molecules and target are available, a docking algorithm with a scoring function is employed to find the compounds in the chemical library that have the highest affinity for the target (e). A visual evaluation of the docking solutions of the ligands

that scored the highest can be performed to confirm their forms of interaction with the active site's critical residues (e). The candidate compounds with the strongest affinity predictions are then considered potential hits and must be confirmed by experimental tests (f). After these studies, the compounds that demonstrate biological activity can proceed to the optimization step, where drug heads can be determined series (g) [4].

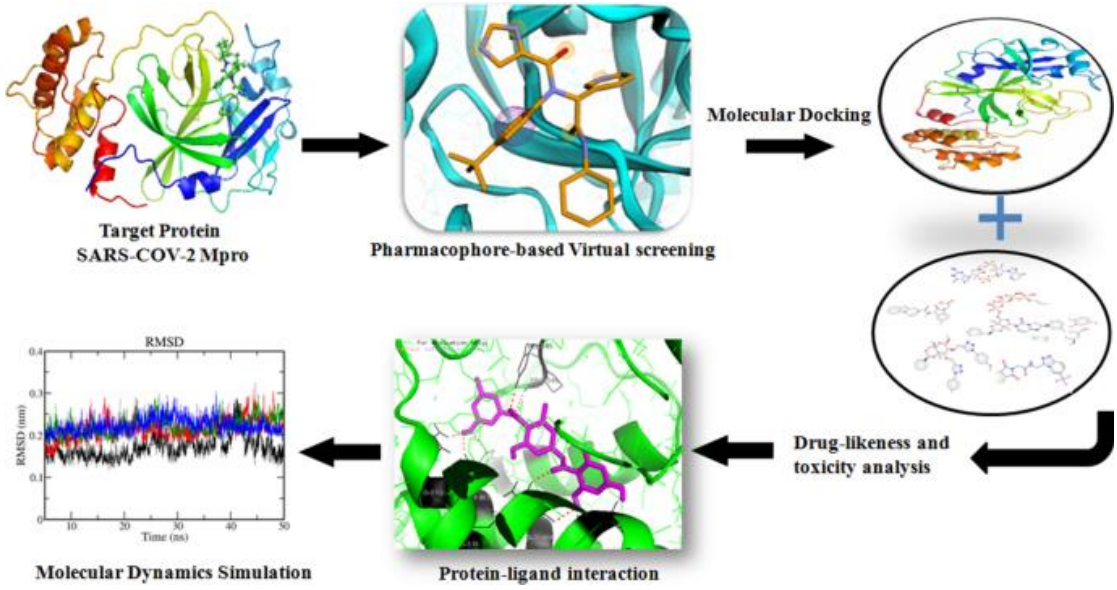

Figure .2. Example of Ligand-based (E-pharmacophore) and structure-based virtual screening steps

- **E-pharmacophore :**

Another tool that has attracted the attention of researchers recently is e-Pharmacophore implemented in phase version 3.0.32,33 It uses a novel methodology and is quite different from other tools in this respect. e-Pharmacophores are structure-based pharmacophores generated by energy optimization of structure-based pharmacophores. They combine the advantages of two principal computational approaches, ie, the computational efficiency of ligand-based pharmacophore screening and the accuracy of scoring from structure-based docking. The methodology begins with refinement of the ligand pose of the ligand-receptor

complex and computation of the Glide XP scoring terms. This is followed by mapping of the energies onto atoms. The next step involves generation of pharmacophore sites, followed by summation of the Glide XP energies from the atoms that comprise each pharmacophore site. Finally, the top scoring sites based on energetic ranking are used to generate a pharmacophore hypothesis that is then used for screening a database. The advantages of this method for virtual screening experiments include better database enrichments, greater diversity of retrieved actives, and faster database screening as compared with other virtual screening approaches. The e-Pharmacophore method leverages the strengths of both approaches to produce high enrichments with good diversity of active molecules. Indeed, the e-Pharmacophore method has been shown to retrieve a more diverse set of actives than other structure-based pharmacophore methods, making it a potent tool for lead hopping.47 Since e-Pharmacophore includes an integrated screening module, there is no need to export data to other screening programs.

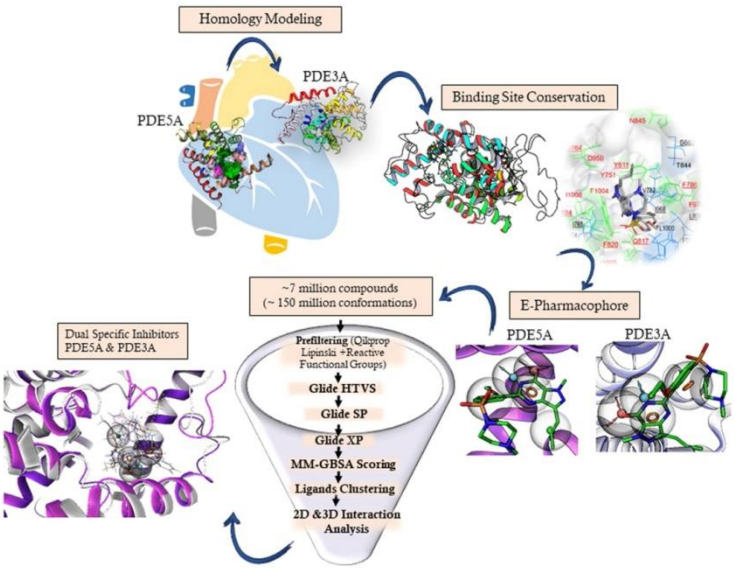

Figure .3. Example of Ligand-basd (E-pharmacophore) and structure-based virtual screening steps

3. Virtual screening tools

3.1. The target

The three-dimensional structure of the target protein utilized in this study is from the PDB. It is the most comprehensive structural database of macromolecules. It was founded in 1971 with just seven constructions. Since then, the number of 3D macromolecule structures has steadily increased, reaching over 110,000 as of June 2015, including 101,300 proteins. The great majority of structures in the PDB are derived by X-ray crystallography, however there are a few structures discovered through NMR and electron microscopy [5].

Certain proteins may not yet be accessible in the database, but if they have comparable sequences, they can be constructed.It is vital to note that certain proteins are not yet accessible in this database, and if the latter has a protein with comparable sequences, it becomes feasible to design the 3D structure of the required target, using homology modeling. [6]

3.2. chemical libraries

Virtual screening is the process of assessing in silico the activity of a large number of compounds towards a certain target. Pharmaceutical businesses have to establish collections to arrange this massive amount of data. These collections are also known as chemical libraries. Currently, there are two sorts of chemical libraries: actual and virtual. Actual chemical libraries are frequently in the form of well plates, each holding a distinct product. These plates are consequently ready for testing. In this study, we are interested in virtual chemical libraries, which are a collection of more or less ordered and hierarchical information that contains all or part of the data on a set of substances. In this type of chemical library, each compound's coordinates are saved

in SMILES, SDF, MOL2, and PDB files. We cite the following virtual chemical libraries: the French National Chemical Library, ZINC, and PubChem [7].

3.2.1. French National Chemical Library

The National Chemical Library, which is supervised by a CNRS service group, was established in 2003 through an agreement between the CNRS and 17 higher education research institutions. It combines the collections of synthetic goods and natural extracts housed in French public laboratories and assures their scientific and economic value. In March 2015, the French national chemical library advertised around 57,000 molecules for sale in bulk or on plates [8].

3.2.2. Pubchem

PubChem consists of three inter-linked databases, Substance, Compound and BioAssay. The Substance database contains chemical information deposited by individual data contributors to PubChem, and the Compound database stores unique chemical structures extracted from the Substance database.

3.2.3.Zinc

This is a database featuring chemicals for sale that are acceptable for virtual screening. It now has over 90 million chemicals that can be purchased easily. This database, managed by the Shoichet Laboratory in the department of pharmaceutical chemistry at the University of California, San Francisco (UCSF), is freely available to all scientists [9].

3.3. The program

Many papers have offered parallel tests conducted with a variety of virtual screening applications (commercial or not). The most popular options are AutoDock Vina, Gold, Flex X, Glide, and Surflex. These systems are based on fragment adjustment, with the first step being to generate a "negative" model of the active site known as

protomol. This model consists of the site's accessible volume and interaction points such as hydrogen bonding sites, charges, or lipophilic sites. These algorithms are also known as fragmentation/reconstruction algorithms since the molecule is initially separated into stiff and flexible linkages. Following that, the rigid components are positioned initially, and the ligand is gradually reassembled, exploring multiple conformations as flexible connections are established This technique enables the quick screening of huge compound libraries [6].

4. Molecular Dynamics

Computational drug discovery accelerates the arduous process of creating and optimizing novel therapeutic candidates. [10].Computational structure-based drug design (SBDD) has had a significant influence on drug discovery over the last decade because to advancements in faster architectures and efficient algorithms for high-level calculations. [11]. Classical molecular dynamics (MD) simulations now provide SBDD techniques that take into consideration the structural flexibility of the drug-target system. [12,13]. The drug-binding paradigms of induced-fit and conformational selection have replaced Emil Fischer's lock-and-key approach.[14-16]. Receptor and ligand flexibility is essential for accurately predicting drug binding and related thermodynamic and kinetic features.[17,18] As a result, conventional MD is no longer regarded a barrier to effective drug creation. Instead, it is pushing the boundaries of computational drug discovery in academia and industry [19]. Classical molecular dynamics (MD) is a physical approach for investigating atom and molecule interactions based on Newton's physics. A force field estimates the forces between atoms and calculates the system's energy. MD simulations use Newton's equations of motion to construct trajectories that define particle locations and velocities throughout time.

4.1 .Dynamic cross-correlation matrices (DCCM)

The cross-correlation is a 3 D matrix representation that graphically visualized the time-correlated pattern of residues of the proteins. The DCCM analysis of the backbone Ca atom in the trajectories was performed to explore the correlation motion between residues of docked complex [20]. The DCCM was computed as the following equation:

$$\mathrm{Cij} = \frac{< \Delta Ri.\Delta Rj >}{\sqrt{< \Delta Ri.\Delta Rj >.< \Delta Ri.\Delta Rj >}}$$

WhereΔRi and ΔRj denote displacement of ith and jth atom from the mean, respectively, and i and j represent ith and jth residues. The coefficient of cross-correlation Cij varies from +1 to -1; the negative value indicates an anticorrelated motion between residues i and j, while positive values indicate a strongly correlated motion between residues i and j within the period of simulations. The DCCM was conducted using Matlab 2016.

4.2 .Binding free energy calculations

The binding free energy of the protein-ligand complex plays an important role in correlating the structure and function of proteins. The MM-PBSA approach was defined by Kollman et al.[21,22]. It is a popular approach to estimate the free energy of the binding of small ligands with protein targets based on MD simulation of the protein-ligand complex. In this study, we have analyzed components of the binding free energy of the protein-ligand complex using the g_mmpbsa tool [23]. In general terms, the binding free energy (ΔGbind) was computed as the following equation:

$$\Delta\mathrm{Gbind} = \mathrm{Gcomplex} - (\mathrm{Gprotein} + \mathrm{Gligand})$$

Where, $G_{complex}$ is the whole free energy of the proteinligand complex; $G_{protein}$ and G_{ligand} are the total free energy of the separated protein and ligand in the solvent,

respectively. The free energy for each individual $G_{complex}$, $G_{protein}$, and G_{ligand}were computed as the following equation:

$G_x = E_{MM}-(TS)+ (G_{solvation})$

Where x represents a protein, ligand, or complex, and E_{MM} represents the average molecular mechanic's potential energy in a vacuum, TS denotes the product of the temperature and entropic contribution, and $G_{solvation}$ is the free energy of solvation. The $E_{MM}$was calculated in vacuum was computed as the following equation:

$E_{MM}= E_{bonded}+ E_{non-bonded}=E_{bonded}+(E_{vdw}+ E_{elec})$

Where, E_{bonded} is bonded interactions, and $E_{non-bonded}$ includes electrostatic (E_{elec}) and van der Waals (E_{vdw}) interactions, respectively. The solvation free energy (Gsolvation) was estimated as the sum of polar solvation free energy (G_{polar}) and non-polar solvation free energy ($G_{non-polar}$) are also called desolvation energy, using an implicit solvation model was computed as the following equation:

$G_{solvation}= G_{polar}+ G_{nonpolar}$

Where, G_{polar} and Gnon-polar are an electrostatic and nonelectrostatic contribution to the solvation free energy, respectively, $_{Gnon-polar}$is estimated from the solvent-accessible surface area (SASA was computed as the following equation:

$G_{non-polar} = \gamma SASA + b$

Where SASA is the change in accessible molecular surface area on binding, and c is a microscopic surface free energy for the solvent, and b is a fitting parameter.

4.3.Free energy landscape (FEL)

In the Landau theory of phase transitions, a thermodynamic potential is given as a function of an order parameter and the state corresponding to a minimum of the thermodynamic potential is realized in equilibrium. It is important in this view to note that the state corresponding to a given value of the order parameter would be realized

under a certain constraint, and that the equilibrium state is realized when the constraint is lifted. For the glass transition, the system cannot be characterized by a small number of order parameters, but it must be specified by the position of all atoms averaged within a certain time scale in which the system keeps its topologically identical structure. Therefore, the free energy relevant to discussion of the glass transition must be considered as a function of atomic coordinates which are constrained by a fictitious field. We define the partial configuration partition function by

$Z(T, V, N, \{Ri\}) = \int ... \int \exp[-\beta\Phi(\{ri\})]\Delta(\{ri - Ri\})d\{ri\}$,…….()

where ri and Ri are the atomic coordinate of ith atom and its position averaged within a certain time scale, respectively. In Eq. (1), T, V, N are the temperature, volume and number of atoms, β = $1/k_BT$ and $\Phi(\{ri\})$ is the potential energy. The gate function $\Delta(\{ri\ Ri\})$ defines the limited space in the phase space where the integration is carried out and is determined by the fictitious field. From the partial partition function, we can define the free energy as a function of {Ri}

F (T,V, N,{Ri})= - k_BT log Z(T , V, N,{Ri})+ contribution of kinetic energy …….(2)which we consider the definition of the free energy landscape. In a practical calculation, we may approximate the gate function by a set of Gaussian field

$\Delta(ri\text{-}Ri) = \sum(\frac{\pi}{\alpha})^{3/2} exp[-x(ri - Ri)^2]$,……(3)

where a is a parameter chosen appropriately. This definition leads to an important concept for the rearranging region in the relaxation process. Consider two adjacent basins in the landscape. The difference between these two basins is given by the position of a few atoms at the local minima which occupy topologically different locations. These atoms can be regarded as a simultaneously rearranged region (SRR).

On the other hand, when the system traverses from one of these basins to the other, it must pass an excited state where much more atoms are involved. The atom at the excited state are not, however, the entire atoms in the system but several atoms surrounding the atoms of the SRR. These atoms are considered as the cooperatively rearranging region (CRR) proposed by Adam and Gibbs [24]. It can be said that the elementary process of relaxation between two adjacent basins occurs within the CRR and the structure of the FEL for the CRR will determine the characteristics of the relaxation process where atoms outside the CRR act as a heat bath. In this view of the construction of the FEL, we expect a almost flat FEL above a certain temperature TC (liquid state) and a ragged one below TC (super-cooled liquid and glass) as schematically depicted in Fig. 1. In the trap model, the glass transition takes place when the average

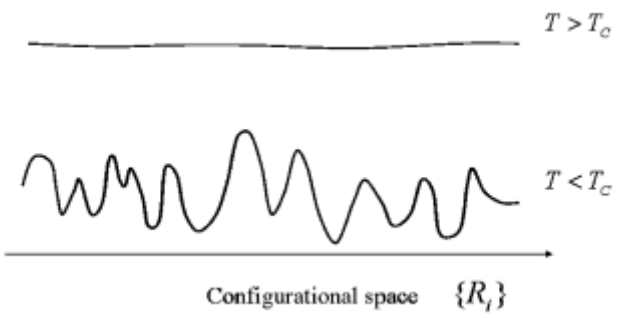

Figure. 4. The expected FEL for high and low temperatures. The jump motion among the basins becomes slower and slower as the temperature is reduced, and when the mean waiting time for the jump motion exceeds the observation time, the glass transition occurs in the trap model.

waiting time for moving out from a basin exceeds the observation time as the temperature is reduced [25].

4.3.1 .Principal component analysis for the free energy landscape

Suppose a system composed of N atoms whose positions at time t are denoted by {ri(t)}. We construct a 3N × 3N variance-covariance matrix A by

A=$< X(t)X^t(t) >$,…… (5)

where(t) is the column vector consisting of ri(t), the superscript t denotes the transposed vector and the average $< \cdots >$ is taken over a sufficiently long period compared to the observation time. We denote eigenvalues and eigenvectors of A by $\lambda$and respectively

$$A\mathbf{v}_\ell = \lambda_\ell \mathbf{v}_\ell. \quad \text{……..(6)}$$

It is known that large k‘’s correspond to slow processes. The projection of x(t) onto v‘ is denoted by y‘(t)

$$\mathbf{y}_\ell(t) = \mathbf{v}_\ell^{\mathrm{t}}\mathbf{x}(t). \quad \text{…..(7)}$$

We can basically analyze the probability distribution $p(y_{\ell_1}, \ldots, y_{\ell_M})$ for a set of slow principal components $y_{\ell_1}, \ldots, y_{\ell_M}$, and the free energy landscape can be defined by

$$F(y_{\ell_1}, \ldots, y_{\ell_M}) = -k_{\mathrm{B}}T \log p(y_{\ell_1}, \ldots, y_{\ell_M}). \quad \text{…… (8)}$$

We performed a constant temperature MD simulation for a model high polymer consisting of bonds and balls. (See Ref. [26] for details.) We picked up two principal components $(y_\ell, y_{\ell+1})$chosen appropriately and obtained the probability distribution $p(y_\ell, y_{\ell+1})$, from which the free energy is determined by Eq. (8). Fig. 3 shows the contour plot of the

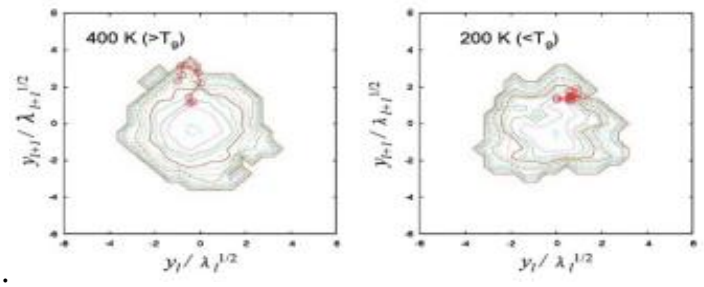

..

Figure.5. Contour of the FEL in two principal axes for a model high polymer (Tg = 230 K) determined by MD simulation. While a single basin is seen at 400 K, two basins exist at 200 K.

FEL for two different temperatures. It is interesting to note that the single basin at 400 K develops into two basins at 200 K which is below Tg.

Réfrences

1. BENCHEIKH, B. In silico screening of SARS CoV 2 inhibitors by molecular docking and QSAR. 2023. Doctoral dissertation.

2. Krid,Y. In silico design of new flavonols potentially inhibiting the Angiotensin Converting Enzyme for the treatment of arterial hypertension. University master's thesis: Molecular Biochemistry and Health. Canstantine: University of the Mentouri brothers. Algeria. 2013. 90.

3. Arrault A. Docking-scoring strategies assisted by data analysis. Application to virtual screening of COX-2 and PPAR gamma therapeutic targets. University doctoral thesis: Molecular Modeling and Chemoinformatics. Orléans: University of Orléans. France. 2007. 176.

4. Martin L. Development of a bioinformatics platform of tools for structural modeling and comparative virtual screening: an application on the protein kinase FAK. University doctoral thesis: Bioinformatics. Montpellier: Montpellier 2 University. France. 2006. 149 p.

5. Protein Data Bank. www.rcsb.org/pdb/home/home.do .04/05/2015.

6. Mokrani,E. H. Contribution to the improvement of the biological activity of dipeptidyl-peptidase 4 inhibitors in type 2 diabetes by computer simulation. University master's thesis: Technology of biochemical explorations. Constantine: Mentouri Constantine University. Algeria. 2012. 75p.

7. Judith,E.K. drug design in silico virtual screening of proteins for therapeutic purposes. University doctoral thesis: Bioinformatics. Montpellier: University of Bordeaux 1. France. 2011. 251 p.

8. The national chemical library. http://chimiotheque-nationale.cn.cnrs.fr/05/18/2015].

9. PubChem.https://pubchem.ncbi.nlm.nih.gov/18/05/2015

10. Jorgensen, W.L. "The many roles of computation in drug discovery." Science 2004, vol. 303, no 5665, p. 1813-1818.

11. DE VIVO, M. Bridging quantum mechanics and structure-based drug design. *Front. Biosci*, 2011, vol. 16, no 5, p. 1619-1633.

12. Durrant, J.; McCammon, J. A. Molecular dynamics simulations and drug discovery. *BMC Biol*. 2011, 9, 71.

13. Harvey, M. J.; De Fabritiis, G. High-throughput molecular dynamics: the powerful new tool for drug discovery. *Drug Discovery Today* 2012, 17, 1059−1062.

14. Boehr, D. D.; Nussinov, R.; Wright, P. E. The role of dynamic conformational ensembles in biomolecular recognition. *Nat. Chem. Biol*. 2009, 5, 789−796.

15. Changeux, J.-P.; Edelstein, S. Conformational selection or induced fit? 50 years of debate resolved. *F1000 Biol*. Rep. 2011, 3, 19.

16. Vogt, A. D.; Di Cera, E. Conformational selection or induced fit? A critical appraisal of the kinetic mechanism. *Biochemistry* 2012, 51, 5894−5902.

17. Fischer, M.; Coleman, R. G.; Fraser, J. S.; Shoichet, B. K. Incorporation of protein flexibility and conformational energy penalties in docking screens to improve ligand discovery. *Nat. Chem*. 2014, 6, 575−583.

18. Abagyan, R.; Totrov, M. High-throughput docking for lead generation. Curr. Opin. *Chem. Biol*. 2001, 5, 375−382.

19. Borhani, D. W.; Shaw, D. E. The future of molecular dynamics simulations in drug discovery. J. *Comput.-Aided Mol. Des*. 2012, 26, 15−26.

20. Ghosh, A., & Vishveshwara, S. A study of communication pathways in methionyl-tRNA synthetase by molecular dynamics simulations and structure network analysis. *Proceedings of the National Academy of Sciences of the United States of America*, (2007),104(40), 15711–15716. doi: 10.1073/pnas.0704459104

21. Kollman, P. A., Massova, I., Reyes, C., Kuhn, B., Huo, S., Chong, L., Lee, M., Lee, T., Duan, Y., Wang, W., Donini, O., Cieplak, P., Srinivasan, J., Case, D. A., Cheatham, T. E. 3rd., &, Calculating structures and free energies of complex molecules: Combining molecular mechanics and continuum models. *Accounts of Chemical Research*, (2000).33(12), 889–897. https://doi.org/10.1021/ar000033j.

22. Srinivasan, J., Cheatham, T. E., Cieplak, P., Kollman, P. A., & Case, D. A.Continuum solvent studies of the stability of DNA, RNA, and phosphoramidate DNA helices. *Journal of the American Chemical Society*, (1998). 120(37), 9401–9409. https://doi.org/10.1021/ja981844þ

23. Kumari, M., & Subbarao, N. Identification of novel multi-target antitubercular inhibitors against mycobacterial peptidoglycan biosynthetic Mur enzymes by structure-based virtual screening. *Journal of Biomolecular Structure & Dynamics*, (2021). 1–12. https://doi.org/10.1080/ 07391102.2021.1908913.

24. ADAM, Gerold et GIBBS, Julian H. On the temperature dependence of cooperative relaxation properties in glass-forming liquids. *The journal of chemical physics*, 1965, vol. 43, no 1, p. 139-146.

25. ODAGAKI, T. Glass transition singularities. *Physical review letters*, 1995, vol. 75, no 20, p. 3701.

26. ODAGAKI, Yuji, KOYAMA, Tsukasa, et YAMASHITA, Itaru. Pharmacological characterization of epinephrine-stimulated GTPase activity in human platelet membranes. *Biochemical pharmacology*, 1993, vol. 46, no 11, p. 2021-2028.

Chapter III: Identification of potent acetylcholinesterase inhibitors as new candidates for Alzheimer disease

1. Introduction

Alzheimer's disease (AD) is a neurological ailment (i.e., progressive brain damage leading to neuronal death) characterized by a gradual loss of memory and some intellectual (cognitive) functions that have implications for daily life activities. Alzheimer's disease would be the leading cause of dementia, accounting for 60-80% of cases [1]. This condition causes a variety of cognitive impairments, including memory loss, cognitive abnormalities, thinking difficulties, language issues, and so on [1, 2].Current research suggests that enhancing brain cholinergic neurotransmission by lowering the chemical reaction of AChE hydrolysis is the most effective treatment for Alzheimer's disease, however the disease's pathogenesis is not fully understood. Acetylcholinesterase (AChE) research in persistent Alzheimer's disease has emerged as a promising avenue of investigation.AChE is an important enzyme in the central nervous system that regulates acetylcholine-mediated neurotransmission. Nowadays, AChE inhibitors, particularly rivastigmine, donepezil, and galantamine, are widely used in the treatment of Alzheimer's disease. In reality, the dependability of these medications is harmed by a variety of adverse effects, including hypotension and hepatotoxicity [3]. Despite the negative effects of AChE-inhibiting pharmaceuticals, this research avenue remains a potential option for developing innovative therapies to treat Alzheimer's disease [4]. Human acetylcholinesterase (hAChE) has a core mixed β-sheet structure with 12 strands and 14 α-helices.

The combination of e-pharmacophore structure-based approaches with molecular docking studies is an extremely successful strategy to drug development.

Pharmacophore-based approaches can identify important molecular properties required for a compound's interaction with a target receptor, which improves our knowledge of the binding requirements. When paired with molecular docking, which

mimics the interaction of a tiny molecule (known as a ligand) and its target receptor, this integrated technique greatly enhances drug discovery [5].

Our key goal during this phase was to predict the affinity between the receptor's interacting amino acid residues. This was done by combining the acetylcholinesterase target protein with an Alzheimer's disease-related ligand, such as a medication or Huperzine.

This approach allows us to determine how well these ligands attach to the enzyme acetylcholinesterase, which is critical in the treatment of Alzheimer's. We next studied the compounds under consideration for ADMET characteristics, determining their potential as prospective therapeutic candidates capable of binding to the acetylcholinesterase protein. This finding offers great promise for the creation of novel inhibitors that might possibly attenuate and hinder the aggressiveness of the hAChE enzyme, which is strongly associated to the course of Alzheimer's disease.

Furthermore, to assess the stability of the produced complexes, we ran molecular dynamics (MD) simulations and calculated many parameters, including the Dynamic Cross-Correlation Matrix (DCCM), Free Energy Landscape (FEL), and Molecular Mechanics Poisson-Boltzmann Surface Area (MM-PBSA).These studies provided a more in-depth insight of the stability and energetics of the ligand-protein complexes, broadening our understanding of their interactions and reaffirming their potential as therapeutic candidates.

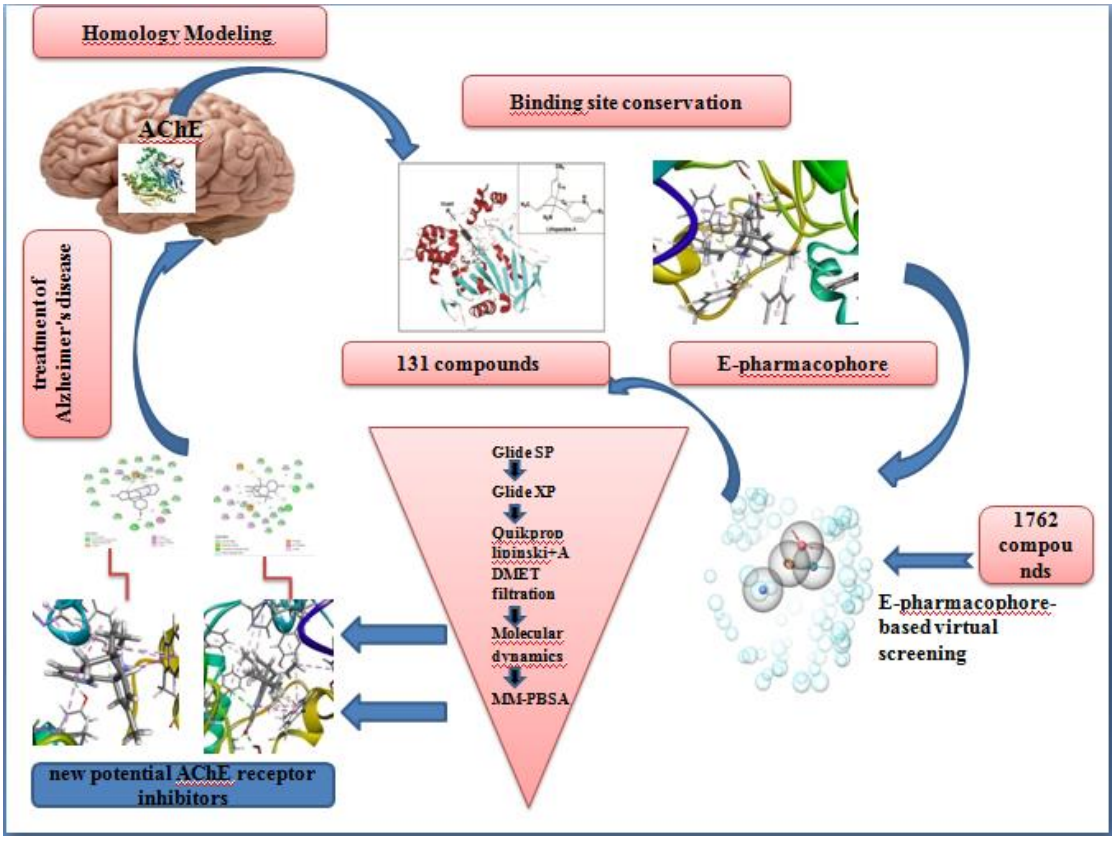

Schematic 1. Representation of the methodologies followed in the present study.

2. Materials and Methods

2.1.Data set

In this work, the data is divided into three parts. The first part contains 39 compounds collected from the literature [6] and used to validate the in silico E-pharmacophore model. The second Contein-900 molecule was obtained from the Dude-Decoys site [7].These molecules have also been used in the validation of in silico E-pharmacophore models. One thousand seven hundred sixty-two molecules, which were derived from Huperzine A and retrieved as SDF files from the PubChem database, were employed for screening and docking through in silico E-pharmacophore models.

2.2.Preparing the Ligand structure

Using the Pub Chem tool https://pubchem.ncbi.nlm.nih.gov/, 3D ligand structures were downloaded in SDF format and were then exposed to Maestro's LigPrep panel in Schrödinger Suite 2018 https://www.schrodinger.com/products/ligprep. The resulting energy-minimized conformers, chirality, and ionized states at pH 7.0 ± 2.0 were preserved, and salts were removed using Epik (4.1); furthermore, LigPrep ensured the exclusion of structurally unwanted ligands. The force field was constructed to minimize the prepared ligands using Optimization Potential Liquid Simulation (OPLS-3). This force field was developed specifically for simulating small molecules.

2.3.Preparing the Protein Structure

The X-ray crystal structure of Acetylcholinesterase (hAChE) forming a stable complex with the inhibitor, accession code Huperzine A (HUP, PDB ID: 4EY5) [8]was retrieved from the RCSB Protein Database. The 3D crystal structure of the enzyme was pre-processed using a Protein Preparation Wizard (Maestro) program (Schrodinger Suite 2018 Protein Preparation Wizard; Epik Schrödinger, LLC: New York, NY, USA, 2018). This step is crucial to ensure that the protein is properly prepared for molecular docking investigations so that it can correct any problems in the protein, for example: remove missing atoms, rings, or side chains as well as unwanted components, and correct the bonding sequence [2].

2.4.Receptor grid generation

Grid boxes can usually be created using the module ‘’receptor grid generation’’. [9].The workspace ligand center of mass has a closed box to represent the activity of the receptor. The process laid out in the'receptor grid generation' module was used to

determine the centers of the bound ligands in the target, resulting in the creation of the grid arrays. of Maestro Glide v8. 3, Schrödinger LLC.

2.5. Development of e-Pharmacophore Hypothesis

The ensemble of steric and electronic properties required to ensure ideal supramolecular interactions with a particular pharmacological target structure and to initiate (or inhibit) its biological response is referred to as a "pharmacophore". The Phase module of the Schrödinger software was employed to exploit and develop E-pharmacophore functions using XP descriptor data [10].The hydrogen bond (HB) donor (HBD), the HB acceptor (HBA), the hydrophobic group (H), the positively and negatively ionizable groups (P) and (N) respectively, and the aromatic ring (R) were used to generate E-pharmacophore sites [11]. These chemical attributes were ranked using the Glide XP estimated energy contribution to anchoring the ligand within the binding pocket. [12] Following that, the created library was screened using the Phase Ligand Screening panel against the generated pharmacophoric characteristics, yielding a collection of compounds that matched the features.

2.6. Enrichment Calculations

The hypothesis was further tested for robustness and the capacity to discriminate between active and inactive substances using enrichment analysis." For this reason, the enrichment calculator program included in the Schrodinger suite was used.

The decoy collection, which included 900 chemicals, was obtained from the DUD: Directory of Useful Decoys database [7].The model's integrity was then tested using the DUD dataset and 39 known acetylcholinesterase inhibitors. Eventually, the query model picked and evaluated the dataset, yielding an array of statistical parameters. The receiver operating characteristic (ROC) curve, the enrichment factor (EF), area under accumulation curve (AUAC), and BEDROC were used to verify the e-

pharmacophore model using prepared data set concatenation [Equations (1)], where the enrichment factor (EF) is described as the proportion of drugs already defined when part of a database is analyzed [13]and the F (X%) is the proportion of known agents returned after screening X% of the database, and we initially focused on EF (1%)[14].Another enrichment metric, Boltzmann-enhanced receiver operating characteristic discrimination (BEDROC), was used to guarantee that pharmacophore results were meaningful[15].To compare these values, we utilized α=8.0, α=20.0, and α=160.9. It was determined that selecting α = 20.0 was an acceptable number for virtual screening.

$$\mathbf{EF} = \frac{\mathbf{Ha \times D}}{\mathbf{Ht \times A}} \text{.....(1)}$$

2.7. Glide Ligand docking

The suggested compounds were glide-docked using previously produced receptor lattices and ligand molecules. To find the best possible interactions between drugs and receptors, the Glide ligand docking program was used. Docking calculations were performed in SP (standard precision) and XP (ultra-precision) [5,16,14], using the OPLS 2005 force field [13]. The docking methodology is carried out in a flexible docking mode that produces conformations for every input ligand automatically. A sequence of hierarchical filters is applied to the obtained ligand positions in order to assess the ligand-receptor interactions. Using a grid-based method based on modelling of the empirical ChemScore function[17], the primary filter assesses the complementarity of the ligand-receptor interaction and the spatial fit of the ligand to the designated active site. The algorithm detects favorable hydrophobic interactions, hydrogen bonding, and metal linkage interactions and penalizes steric conflicts. Poses that meet these basic criteria go on to the last step of the algorithm, where the lattice-approximate OPLS interaction energy between the unbound ligand and receptor is

assessed and minimized. Lastly, the glide score scoring function is used to rescore the minimization posture. The XP-Glide scores of the active compounds were consolidated, and the fitness scores of each ligand were compared. The docking results were analyzed using Biovia Discovery Studio. 4.5.12 http://www.3dsbiovia.com.

2.8.Structure-based virtual screening

Virtual screening is a powerful methodused to find active ingredients or lead molecules and has been incorporated into the drug discovery process of several pharmaceutical companies. These active site screening studies were performed using Schrödinger Suite, E-pharmacophore and docking virtual screening workflows. For the electronic pharmacophore approach, it is necessary to identify the most favorable sites for the distribution of energy (superior to 1.0 kcal mol^{-1}).When screening molecules, at least four sites must match the hypothesis. The distance adjustment tolerance is set at 2.0 in order to achieve a harmonious equilibrium between tight and loose alignment. The database hits are arranged in order of their fitness score, which is a measure of how well the aligned ligand conformers match the hypothesis. This evaluation considers factors such as RMSD position agreement, vector alignment, and volume parameters. The fitness score function is an equally weighted combination of these three terms, ranging from 0 to 3, as implemented in the standard database filter in Phase Phase, version 3.3, Schrödinger, LLC, New York, NY, 2011.After the pharmacophore-based screening, as indicated by the finess score, the best 131 hits were chosen for molecular docking investigation.

2.9.In silico ADMET prediction

After identifying the besthits using pharmacophore-based virtual screening and molecular docking investigations, we were interested in finding the ADMET

(absorption (A), distribution (D), metabolism (M), excretion (E), and toxicity (T)) properties of the identified compounds. Whether they exhibit drug-like properties was the next question we tried to answer using another tool called QikProp [18]. The QikProp module version 5.4 of Maestro, Schrödinger was used to calculate molecular descriptors (excipients, physicochemical, biochemical, pharmacokinetic, and deleterious properties) and predict the ADMET profiles of these compounds. The SwissADME data sitewas used to calculate the bioavailability score and the synthetic accessibility values http://www.swissadme.ch/. Toxicity refers to the degree to which a substance causes damage to an organism or its underlying structures. Compound toxicity prediction is important to reduce the cost and effort required for preclinical and clinical studies of drugs [19]. Toxicity assessment was also performed using the ProTox platformhttps://tox-new.charite.de and ADMETlab2.0.It gives anticipated harmfulness values, cytotoxicity, mutagenicity, andcancer-causingfeatures of chosen compounds.

2.10.Molecular Dynamics Simulation (MDS)

The biomolecular stability of the generated complexes was assessed through molecular dynamic simulations for 100 ns using Gromacs-2023 on a GPU system.In this phase, the two best hit-molecules **(CID_162895946 and CID_44461278)**were chosen due to their good binding affinities to human Acetylcholinesterase and their pharmacokinetic features.We subsequently simulated the complex Acetylcholinesterase_Huperzine A as a reference complex, considering the same parameters.TheSwissParam platform was employed to create the topology data of the selected hit-molecules [20].In addition, the Acetylcholinesterase topology file was also created using the CHARMM27 all-atom force field[21,22].After generating topology files, each system was immersed (solvated) in a cubic box using the

transferable intermolecular potential with three points (TIP3P) water model. Additionally, Na+ and Cl- ions were introduced to balance the overall charge. The energy of each neutralized system was reduced to a minimum by using the steepest descent and conjugate gradients methods until the maximum force exerted on the system was below 10.0 kJ/mol.The v-rescale approach was used to couple each system at a temperature of 300 K for 100 ps, with a coupling value of 0.1 ps, during the NVT equilibration phase. Subsequently, the NPT equilibration phase was carried out for 100 psutilizing a Berenson pressure-coupling system with a coupling constant of 2.0 ps. [23, 24].

To understand the biomolecular stability and dynamics of the hit-molecules within the human Acetylcholinesterase active site and their effects on its vital and biological functions, the main parameters were evaluated.The root mean square deviations (RMSD) have been employed to determine the changes in the backbone atoms of human Acetylcholinesterase.The root mean square fluctuations (RMSF) were used to quantify the relative variations of each amino acid. The radius of gyration (Rg) is used to figure out the overall compactness. To assess the overall stability of the generated complexes, we calculated the solvent accessible surface area (SASA).

2.11.Dynamic Cross-Correlation Matrix (DCCM)

In order to analyze the collective movements of the studied systems, the gmxcovar tool was used to generate the dynamic cross-correlation matrix (DCCM), which represents the shifts of proteins' C_α atoms during a dynamic time[25].A covariance matrix measuring the correlated aspect of atomic shifts was constructed between atoms *i* and *j*. The cross-correlation can be calculated using the subsequent equation[26]:

$$DCCM_{(i,j)} = \frac{\langle \Delta ri X \Delta rj \rangle}{\sqrt{\langle \Delta ri^2 \rangle}\sqrt{\langle \Delta rj^2 \rangle}} \text{.....(2)}$$

Wherein *Δri* and *Δrj* refer to molecular movement vectors representing atoms *i* and *j* from their average location regarding period interval.

2.12.Free energy landscape (FEL)

Using the conformation sampling technique, the protein's native structural configuration was determined. For the purpose of generating the free energy landscape, we employed two critical components as reaction coordinates in our investigation: structural deviation and protein gyration.The energy landscape was computed with the two aforementioned components, applying the following equation[27]:

$$\Delta G(p1,p2) = -k_B T ln\rho(p1,p2) \text{.....(3)}$$

Where$k_B$is the Boltzmann constant and ΔG represents the Gibbs free energy of state, , and T signifies the simulation temperature.The two-dimensional free-energy landscapes were produced using the system's joint distributions of probabilities, ρ(p1,p2), using two separate response coordinates, p1 and p2.

2.13.Binding Free Energy Calculations

One of the most prevalent methods for determining the binding free energy of a protein-ligand complex is the Molecular Mechanics Poisson-Boltzmann Surface Area (MM-PBSA)[28]. The approach defined in the g_mmpbsa tool has been employed in order to conduct the binding free energy (ΔG_{bind}) assessment for the MM-PBSA[29]. The bindingfree energy is calculatedin the following manner:

$$\Delta G_{bind} = G_{complex} - (G_{protein} + G_{ligand}) \text{.....(4)}$$

Where $G_{Complex}$ represents the binding energy of native protein, $G_{protein}$ and G_{ligand} are the binding energy of protein and ligand.

4. Results and discussion

4.1.Development of e-pharmacophore hypotheses

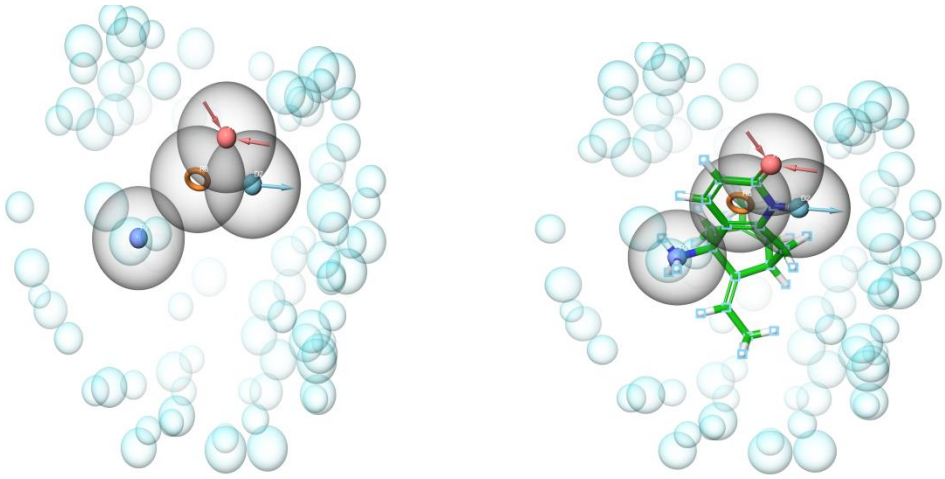

(A) **(B)**

Figure 1.**(A)** Alignment of e-pharmacophore models of Acetylcholinesterase.

(B) Alignment of e-pharmacophore models of Acetylcholinesterase with the referenceligand(HUP).

E-Pharmacophore screening methods, renowned for their swiftness, serve as ideal tools for the preliminary screening of extensive molecular libraries. This strategy entails swiftly identifying top-tier molecules through this rapid approach. These selected compounds are then subjected to a more precise, albeit slower, method such as Glide SP or other comprehensive techniques to determine binding free energy accurately.

To gain an in-depth understanding of inhibitor binding to acetylcholinesterase (AChE), we constructed a structure-based pharmacophore model utilizing the acetylcholinesterase-hup complex.By mapping Glide XP energetic terms onto pharmacophore locales—which were determined based on structure and energy data between the protein and the ligand—e-pharmacophore hypotheses were generated from the re-docked structure of HUP ligand in acetylcholinesterase. The e-

pharmacophore hypothesis created for the 4EY5 catalytic area consisted of four pharmacophore highlights with 2.00 Å distance, which included one hydrogen bond donor (D2), one hydrogen bond acceptor (A1), one aromatic ring (R8), and one ionizable group (positive Ionic) (P7). **Figure 2** shows the selected e-pharmacophore for the crystal ligand contemplated and CID_ 44461278, CID_162895946, CID_44285285 and CID_81108419ligands.

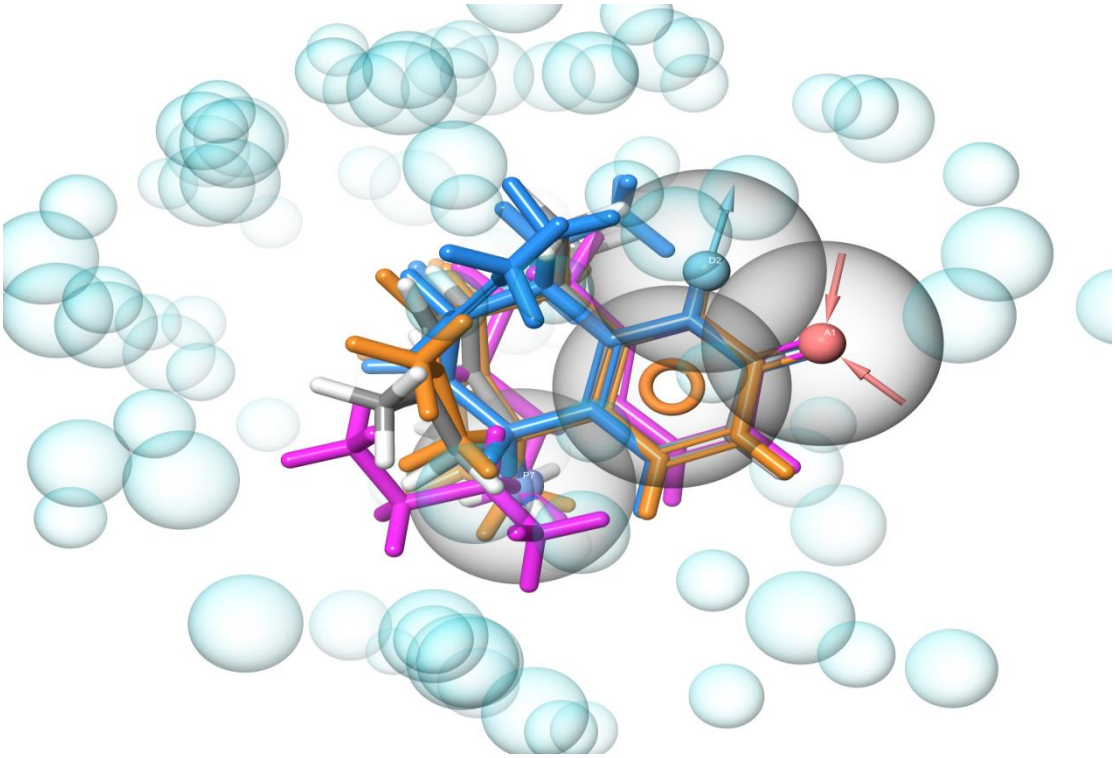

Figure .2. Alignment of respective e-pharmacophore models of 4EY5 with blue color: CID_162895946, graycolor: CID_44461278, orange color: CID_44285285, mauve color: CID_81108419

4.2.Enrichment Calculations

We used the enrichment survey to eliminate pharmacophores lacking meaningful interactions and to focus on pharmacophores for additional virtual screening. Subsequently, we obtained great enrichment and great variety in our hits.

Table 1. Validation of e-pharmacophore model

Metrics	EF (1%)	BEDROC	ROC	AUAC
Values	2.40	0.08	0.70	0.69

Multiple metrics, such as EF, ROC, AUC, and BEDROC were used to validate the model. The EF (1%) score of 2.40 is the greatest rate of active recovery from the dataset in comparison to a randomselection. Furthermore, ROC and AUAC values of 0.7 and 0.69**(Table 1)**indicate that the model is capable of recovering all actives from the decoy set. The ROC plot is depicted in **Figure 3**.It is important to note that the model's BEDROC value was judged to be 0.08, emphasizing its high quality and efficiency in the screening process.Based on the validation results, we think that this E-pharmacophore model is trustworthy and might be used to identify possible hits thoroughly.

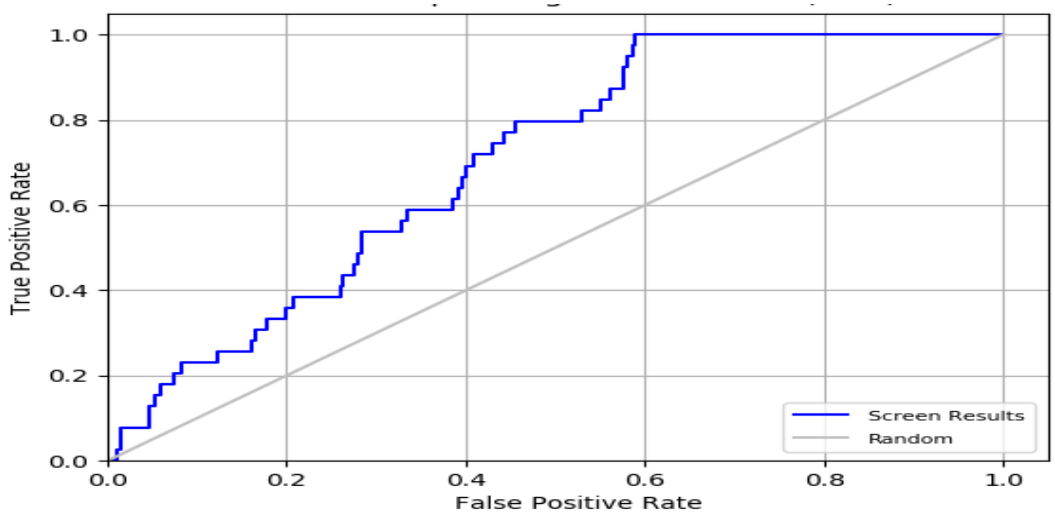

Figure .3. Sketch of the ROC plot used for Validation of e-pharmacophore model

4.3.E-Pharmacophore-based Virtual Screening

We embarked on a quest for new compounds with the potential to serve as potent acetylcholinesterase inhibitors, aiming to address the pressing needs in Alzheimer's research. Leveraging data from the PubChem database, we gathered compounds analogous to our reference molecule (Huperzine A), underpinned by the principle that structural similarity implies shared properties. Our initial step involved employing a validated pharmacophore model, which robustly confirmed its efficacy. This model served as our filter, sifting through a pool of 1762 compounds.

Following stringent screening based on feature count and fit values (more than 2.0), we narrowed down our selection to 131 compounds. This rigorous computational filtration process represents our foundational stride towards identifying promising candidates that could exhibit desirable inhibitory properties against acetylcholinesterase, a critical pursuit in the quest for novel therapeutics targeting Alzheimer's disease.

4.4.Glide Ligand docking

After filtering via the pharmacophore model, a pool of 131 potential compounds was identified. Our subsequent step involves immersing ourselves in docking studies, as delineated in Section 2.3, with the protein 4EY5 serving as our study's focal point. To validate our approach, we initially conducted redocking of the co-crystallized ligand at its stated binding site [30]. By comparing the resulting pose with the reported one, depicted in **Figure. 5**, we confirmed the fidelity of our docking process by computing the Root Mean Square Deviation (RMSD) value. Notably, the RMSD value between the co-crystallized ligand and the re-docked ligand was found to be less than 0.1, affirming the accuracy of our docking methodology.

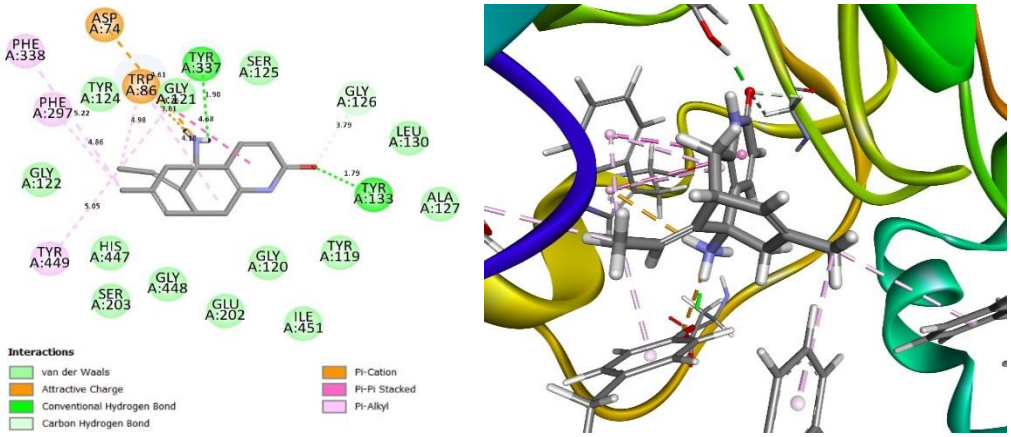

Figure 4.The reference ligand in the active site of the target Acetylcholinesterase and it's interactions with amino-acid residues.

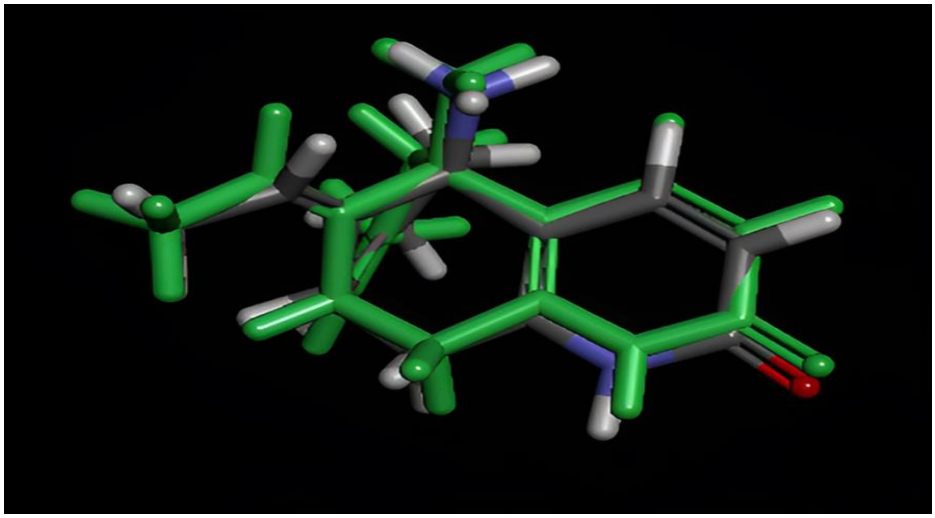

Figure .5.Superimposition image of the X-ray native pose of co-crystal ligand (HUP) and it's re-docked pose of the co-crystal ligand in the active site of the target PDB-4EY5.Gray color: X-ray native pose,Green color: Re-docked pose.

A total of 131 molecules underwent initial screening based on their dock scores, yet all 131 were deemed excessively large for further docking in the higher accuracy mode (XP). Consequently, the initial refinement was carried out through docking in standard accuracy (SP) mode, narrowing down the selection to 40 compounds. SP docking, requiring less CPU time and utilizing fewer scoring terms than XP, provides a computational advantage. While the receptor in grid-based docking remains

primarily rigid, SP mode allows flexibility by scaling specific potential components, enhancing adaptability. Conversely, the XP docking approach serves to eliminate false positives, establishing a robust correlation between favorable poses and high ratings.

Following this screening, molecular XP docking was done on the selected 40 compounds using the 4EY5 crystal structure. Subsequently, four compounds exhibiting the most favorable docking scores (-11.436 to -10.680 kcal/mol) and Glide energies (-55.585 to -38.552 kcal/mol) were singled out for further investigation, as delineated in **Table 2**.The ligands were classified based on their docking scores, and their interactions with unbound amino acids were similar to those of co-crystallized ligands (C15H18N2O, Huperzine A).As illustrated in **Figure 4**, the co-crystallized Huperzine A (HUP) ligand showed a conventional hydrogen bond with TYR 133 and TYR337,Pi-Cation and Attractive Charge with ASP 74 and TRP 86,Pi-Alkyl with PHE 338,PHE 297, TYR 449,TRP 86 ,TYR 337,Carbon Hydrogen Bond with GLY 126 amino acid residue ;considering that the glide energy value of the given molecule is -46.720 kcal/mol and the docking score is -10.217kcal/mol **(Table 2)**.The results obtained about the enzyme's active site, where the ligand binds, and the nature of that interaction are also supported by the literature [6].

The resultant hits of screening with XP docking were further analyzed to gain insight into the binding pattern with the 4EY5 protein.The docking score for the four ligands CID_162895946, 44461278,44285285 and 81108419 was greater than of the co-crystallized ligand (Huperzine A-10.217 kcal/mol).Compounds CID_162895946 and 44461278 which had the highest fitness score (2.900, 2.889respectively) also showed the highest docking score of -11.436 and -11.107kcal/molrespectivly, with a glide energy of -38.552and -50.035 kcal/mol respectively, such Lower values indicate that the inhibitor or activator fits in the actual binding site of the target enzyme and that a stable ligand-receptor complex is formed ; also, both of thesetwo top hits interact with the majority of key residues involved in substrate binding **(Figure 6)**.

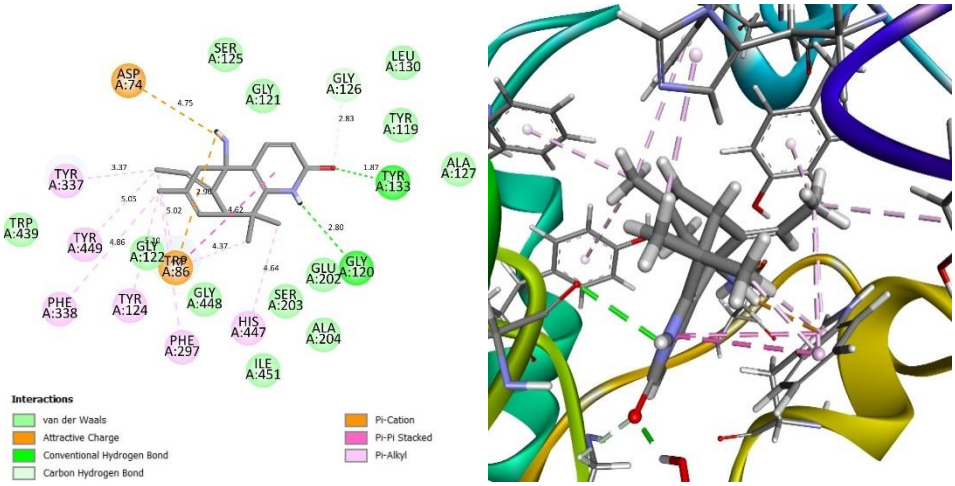
SER A:125
ASP A:74
GLY A:121
GLY A:126
LEU A:130
TYR A:119
TYR A:337
TYR A:133
ALA A:127
TRP A:439
TYR A:449
GLY A:122
TRP A:86
GLY A:120
GLU A:202
PHE A:338
TYR A:124
GLY A:448
SER A:203
HIS A:447
ALA A:204
PHE A:297
ILE A:451
Interactions
van der Waals
Attractive Charge
Conventional Hydrogen Bond
Carbon Hydrogen Bond
Pi-Cation
Pi-Pi Stacked
Pi-Alkyl

(A)

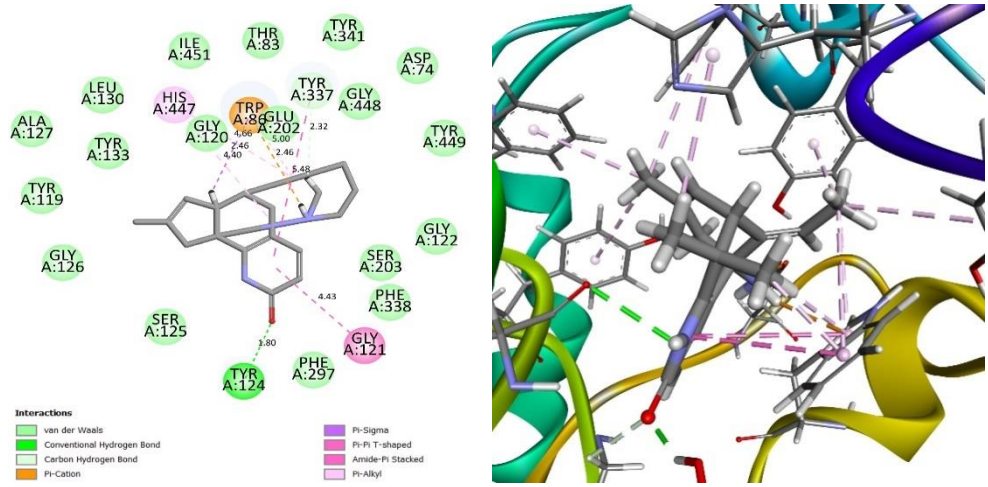
ILE A:451
THR A:83
TYR A:341
ASP A:74
LEU A:130
HIS A:447
TYR A:337
GLY A:448
TRP A:86
GLU A:202
ALA A:127
GLY A:120
TYR A:133
TYR A:449
TYR A:119
GLY A:122
GLY A:126
SER A:203
PHE A:338
SER A:125
GLY A:121
PHE A:297
TYR A:124
Interactions
van der Waals
Conventional Hydrogen Bond
Carbon Hydrogen Bond
Pi-Cation
Pi-Sigma
Pi-Pi T-shaped
Amide-Pi Stacked
Pi-Alkyl

(B)

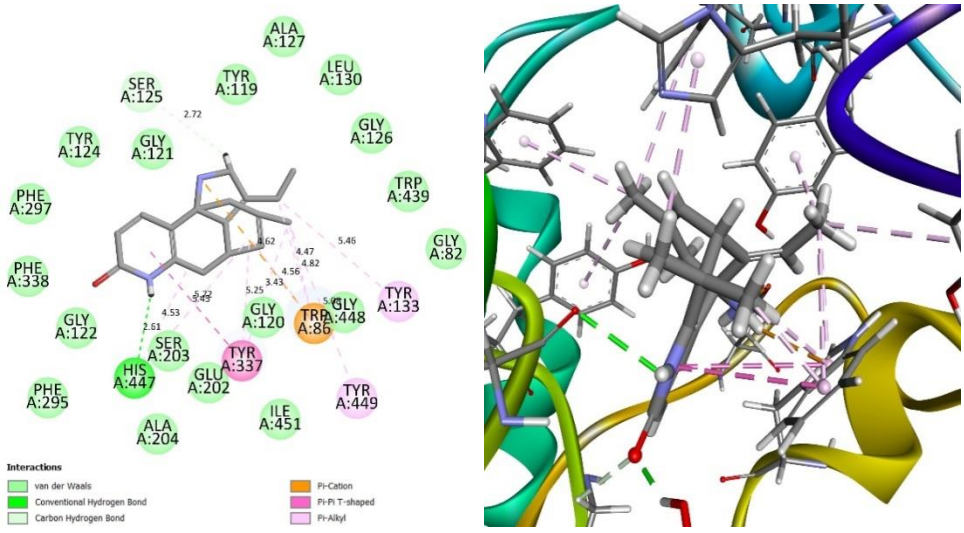
ALA A:127
LEU A:130
SER A:125
TYR A:119
GLY A:126
TYR A:124
GLY A:121
TRP A:439
PHE A:297
GLY A:82
PHE A:338
TYR A:133
GLY A:122
GLY A:120
TRP A:86
GLY A:448
SER A:203
TYR A:337
HIS A:447
GLU A:202
PHE A:295
TYR A:449
ILE A:451
ALA A:204
Interactions
van der Waals
Conventional Hydrogen Bond
Carbon Hydrogen Bond
Pi-Cation
Pi-Pi T-shaped
Pi-Alkyl

(C)

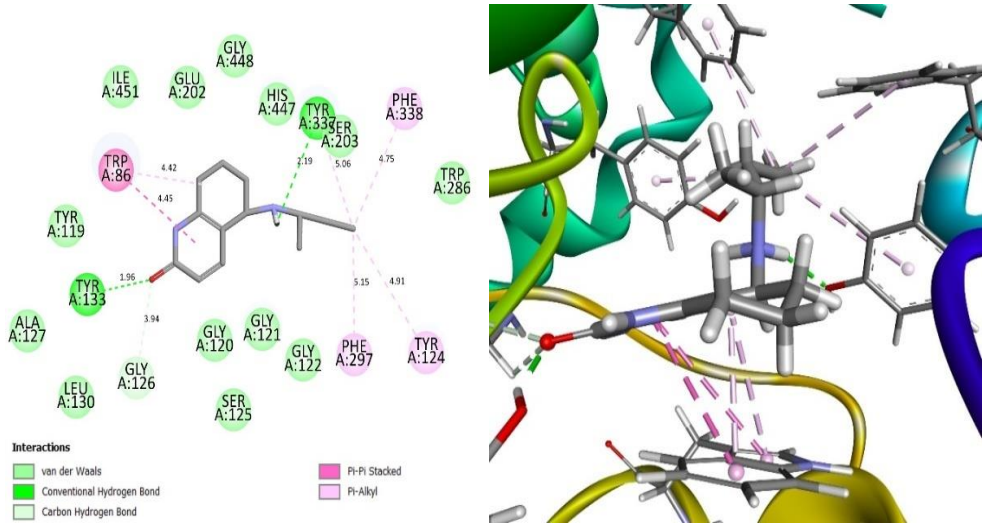

(D)

Figure .6. Interactions between amino-acid residuesand selectedmolecules**(A)**CID_44461278,**(B)** CID_162895946,**(C)** CID_CID_44285285, **(D)**CID_81108419,in the active site of the target 4EY5.

Table 2.Structure, molecular formula, Docking score (SP,XP)kcal/mol, Glide energy andfitnessscore of selected 4 compounds andreference ligand.

Hits	Compound structure	Molecular formula	Docking score(SP) kcal/mol	Docking score (XP) kcal/mol	Glide energy kcal/mol	Fitness score
CID_162895946	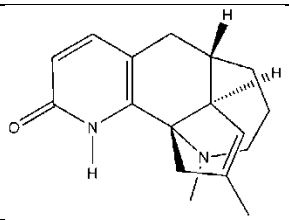	C17H22N2O	-11.387	-11.436	-38.552	2.900
CID_44461278	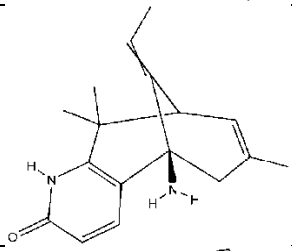	C17H22N2O	-11.026	-11.107	-50.035	2.889
CID_44285285	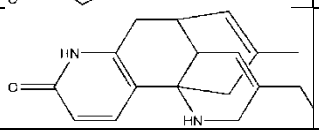	C17H20N2O	-10.724	-10.792	-40.765	2.754

CID_81108419	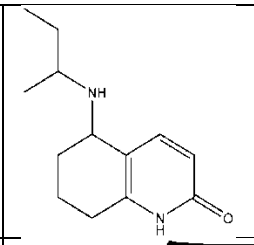	C13H20N2O	-10.672	-10.680	-55.585	2.244
, huperzine A	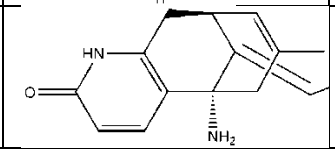	C15H19N2O	-10.120	-10.217	-46.721	///

As illustrated in **Table 3,**CID_44461278 showed a strong conventional Hydrogen Bond, carbon Hydrogen Bond interactionswith TYR 133,GLY 120,Gly 126 amino acid residuesinthe active site of the target and oxygen and nitrogen of the backboneatom;italso showed Pi-Cation interaction and attractive charge with ASP 74 and TRP 86 residues, height Pi-Alkyl interaction with PHE 338, PHE 297, TYR 449 and a view one interaction of the Pi-stacked type (aromatic interactions).

CID_162895946 showed one hydrogen bond and carbon Hydrogen bond interactionswith TYR 124 and TYR 337. Whereas, GLY 121, TYR337 established the Amide Pi-stacked (aromatic interactions) with theCID_1628959446. Pi-Alkyl and Pi-Cation interaction were also observed between the proposed ligand and TRP 86, HIS 447.the Pi-Sigma interaction observed with TRP 86 amino acid residues.

Similarly, the compound CID_44285285showedonehydrogen bond with HIS 447,onecarbonHydrogen Bond with SER 203, ninePi-Alkyl interactions withTYR 133, TYR 449, TRP 86,TYR 337,HIS 447,one Pi-cation with TRP 86 and one Pi-Pi T-shaped with TYR 337amino acid residues.

On the other hand, the compound CID_81108419forms twoconventionalhydrogenbondswith TYR 337, TYR 133, five Pi-Alkyl with SER203, TYR 124, PHE 338, PHE 297, TRP 86, one carbon Hydrogen Bond with GLY 126, one Pi-Pi stacked with TRP86 interactions with amino acid residues.

In addition, by comparing the four structuresof the proposed hits with the structure of the reference ligand, we found that when carbon chains (closed or open) are added to the structure of the reference ligand, the resulting compounds become more stable, and thus the drug effectiveness increases. Thus, we can say that carbon is an essential element for increasing drug effectiveness. When we changed the aromatic ring basic structure of the reference ligand by an open carbon chain (propane) linked to an amine to form an isopropyl amine, we also found that the stability was high, so we can also say that the amine function is essential for the increase in the selected biological activity of the compound.

Table 3.Representations of molecular interactions between CID_ 44461278, CID_162895946, CID_44285285 and CID_81108419ligandsand Acetylcholinesterase receptor.

Compound Code	Residues	Interaction type
CID_ 44461278	TYR 133 GLY120	conventionalHydrogen Bond
	GLY 126	carbone Hydrogen Bond
	TRP 86	Pi-Cation interaction
	ASP 74	Attractive Charge
	HIS 447 PHE 297 TRP 86 TYR124 PHE338 TYR 449 TYR 337	Pi-Alkyl interaction
	TRP 86	Pi-stacked type
CID_162895946	TYR124	ConventionalHydrogen Bond
	TYR 337, GLY 121	Amide Pi-stacked
	HIS447, TRP 86	Pi-Alkyl interaction
	TRP 86	Pi-Cation

	TYR 337	carbonHydrogen Bond
	TRP 86	Pi-Sigma
CID_44285285	HIS 447	ConventionalHydrogen Bond
	SER 125	carbonHydrogen Bond
	133, TYR 449, TRP 86, TYR 337,HIS 447	Pi-Alkyl interaction
	TYR 337	Pi-Pi T-shaped
	TRP 86	Pi-Cation
CID_81108419	TYR 337, TYR 133	ConventionalHydrogen Bond
	SER203, TYR 124, PHE 338, PHE 297, TRP 86	Pi-Alkyl interaction
	TRP 86	Pi-Pistacked

4.5.In silico ADMET predictions

Four best-found hits from virtual screening and molecular docking were exposed to ADMET examination involving the QikProp module in Maestro and ADMETlab data base.QikProp toolswere used to investigate drug-like behavior by analyzing absorption, distribution, metabolism, and excretion (ADME) as well as other pharmacokinetic characteristics **(Table 4)**.

The proposed compounds for Alzheimer's treatment in our case exhibit small molecular masses. Generally, Alzheimer's drugs are typically small in size. This is because these drugs are designed to target specific regions in the brain, aiming to modify chemical processes, enhance cognitive functions, and decelerate disease progression. Their smaller size allows them to efficiently access crucial brain areas, amplifying their impact and efficacy in mitigating symptoms associated with Alzheimer's disease.

The observed range of partition coefficient of the lead compounds (QPlogPo/w) values, from 1.521 to 2.596, is promising. It highlights a well-balanced combination

of hydrophilic and hydrophobic properties crucial for efficient absorption and distribution within biological systems [31]. This balance indicates optimal permeability,which is essential for a drug's effective uptake and potential bioavailability. In the context of Alzheimer's disease, such favorable partition coefficients become pivotal characteristics for evaluating a compound's potential effectiveness as a drug candidate.The projected apparent Caco-2 cell permeability factor QPPCaco, measured in nm/s^{-1}, exhibited values ranging from 226.689 to 633.027 among these hits. This factor is crucial in estimating cell permeability across biological membranes. Notably, the lead compounds from the PubChem library displayed substantial values across the evaluated criteria, demonstrating drug-like characteristics based on various physicochemical parameters.

In general, the compounds' % human oral absorption ranged from 80.541 to 92.287, and their water solubility (QPlog S) ranged from -3.199 to -2.033.pMDCK (cell permeable parameter) values ranged from 110.034 to 333.880 and were used as a model to evaluate the human intestinal barrier and medication absorption efficiency.p log HERG (K+ channel blockage) values were found to be less than 5.The QPlogBB ¼ The predicted brain/blood partition coefficientpenetration numbers given show molecules' capacity to pass the blood–brain barrier (acceptable range: -3 to 1.2).The predicted brain/blood partition coefficient ranged from -0.055to 0.444,demonstrating a greater possibility of BBB penetration.The VD (volume distribution) is an important parameter in our research because the novel chemicals act at the level of the central nervous system; it’s estimated in L/kg.The average VD ranges from 0.04 to 20 L/kg; all compounds have VD values that fall within this required range, indicating that they are properly distributed throughout the body **(table 6)**.Cytochrome P450s are required for medication safety, persistence, and bioactivation. CYP3A4 is the most significant

enzyme in the cytochrome P450 family. More than half of all clinically used drugs interact with it. All compounds have a positive response in the P450 CYP3A4 substrate. As a result, the target ligands have no problems with metabolism or removal.

According to the QikProp ADMET investigation, every compound meets the standard of five with 0 violations (Lipinski's criteria), and the 0.55 bioavailability score validates these compounds' good bioavailability.All of the recently discovered acetylcholinesteraseinhibitors have synthetic accessibility scores ranging from 3.19 to 4.47, indicating that these compounds are easily synthesized, In order to enhance our understanding of the ADME properties, we utilized the AdmeLab software and incorporated the results to support our analysis in TableS1. We observe that all compounds have a low T 1/2 (Half Life Time) with a value <3h indicating that the presented compounds are easily and rapidly cleared from the human body[32].

Table 4.Estimated physicochemical and pharmacokinetic parameters, Bioavailability Score, Synthetic accessibility properties by QikProp and SwissADME

Hits	MW g/mol	lipinsky	QP log Po/wb	QP log S	QP log HERGd	QPPCacoe	QPPMDCK	% of humanoral absorption	Q Plog BBd	Bioavailability Score	Synthétique accessibilité
CID_162895946	270.374	0	2.596	-2.958	-4.438	633.027	333.880	92.287	0.444	0.55	4.46
CID_44461278	270.374	0	2.079	-2.934	-4.734	226.689	110.034	81.277	-0.054	0.55	4.47
CID_44285285	268.35	0	2.265	-3.199	-4.952	246.804	120.624	83.028	-0.046	0.55	4.46
CID_81108419	220.31	0	1.521	-2.033	-4.709	313.894	156.427	80.541	-0.055	0.55	3.19
huperzine,A	242.320	0	1.494	-2.332	-4.706	175.952	83.674	75.880	-0.142	0.55	4.30

MW is the molecular weight; QPlogPo/w is the octanol/water partition coefficient; QPlogS is the projected aqueous solubility; log S: S in moles/l is the concentration of the solute in a saturated solution that is in equilibrium with the crystalline solid.QPPCaco is the projected apparent Caco-2 cell permeability in nm/s; Caco-2 cells are a model for the gut-blood barrier. Recommended values: QPPCaCo = <25 POOR, >500 GREAT. QplogHEGd: Predicted IC50 value for blocking HERG K+ channels. QploghEGd is expected below -5. Predicted apparent MDCK cell permeability in nm/sec (<25 poor, >500 great).QPlog BB is the expected brain-blood partition coeffient; Percent Human-Oral Absorption = <20

POOR, >80great; QPlogBB = −3.0 to 1.2; *Recommended settings - As per the criteria provided in Schrodinger's Maestro software package documentation.

All lead compounds met the pharmacokinetic characteristics for a drug-like molecule and were deemed safe for human consumption. ADMET results have been arranged in **Table (4, 5 and 6)**.We utilized the web-based tool Protox-II to predict the toxicity of the lead compounds. The computerized prediction of toxicity was based on five different targets associated with adverse medication responses. The compounds' hepatotoxicity, carcinogenicity, mutagenicity, cytotoxicity, and LD50 (LD50 of acute toxicity) were anticipated. The four chemicals were found to be almost non-toxic, with an LD50 value greater than 500 mg/kg **(Table 5)**.This research demonstrates that it is possible to boost the biological activity of a natural substance by making a slight structural alteration. The study identifies the sort of alteration that imparts higher AChE inhibitory efficacy to the product, namely a lipophilic substituent capable of making extra hydrophobic interactions with the enzyme.

Table 5. Toxicity prediction of the reference compound and selected hits using Protox-II

Hits	Hepatotoxicity	Carcinogenicity	Mutagenicity	Cytotoxicity	LD50 (LD50 of acute toxicity)
CID_1628959446	Inactive	Inactive	Inactive	Inactive	528.406 mg/kg
CID_44461278	Inactive	Inactive	Inactive	Inactive	550.767 mg/kg
CID_44285285	Inactive	Inactive	Inactive	Inactive	524.467 mg/kg
CID_81108419	Inactive	Inactive	Inactive	Inactive	948.519 mg/kg
huperzine,A	Inactive	Inactive	Inactive	Inactive	225.109 mg/kg

Furthermore, because the predicted log P of analogues is 0.519 to 2.596 against 1.494 for Huperzine, the novel analogues may have a better therapeutic profile due to their greater capacity to cross the blood brain barrier.

Table .6.ADMET properties of reference compound and selected hits using AdmeLab

Hits	**VD (Volume Distribution)**	**P450 CYP3A4 substrate**	**T 1/2 (Half Life Time)**

CID_162895946	0.891 L/kg	++	1.682 h
CID_44461278	0.486 L/kg	+	1.793 h
CID_44285285	0.812 L/kg	+	1.719 h
CID_81108419	0.772 L/kg	+	1.328 h
Reflig	0.424 L/kg	+	1.627 h

4.6.MD Simulations

RMSD and RMSF Analysis

First, we calculated the difference in the structural stability of the three systems' backbone atoms using the RMSD metric.The RMSD values of the examined complexes were compared to the RMSD profiles of the reference complex (Acetylcholinesterase_HUP) and the protein backbone atoms.**Figure.7.** illustrates the RMSD profile of each examined system.It is observable that the RMSD profileof the Acetylcholinesterase_44461278 complex is significantly more stable over 100 ns of Simulationwith an average RMSD of 0.100 nm than the reference complex and protein backbone atoms (with RMSD averages of 0.138 and 0.156 nm, respectively).At the biomolecular level, the compound 44461278 forms a highly stable complex with the Acetylcholinesterase active site, permittingitsselectivityto block the vital and biological activities of this protein.Furthermore, the Acetylcholinesterase_162895946 complex was comparatively stable in the first 55 ns of the simulation. Following this period, the RMSD values approached 0.5 nm in certain cases until the simulation ended. In addition, the average RMSD value of this

complex was 0.138 nm. Finally, RMSD analysis indicates that the identified compounds in this study have the potential to be candidates for Alzheimer's disease treatment.

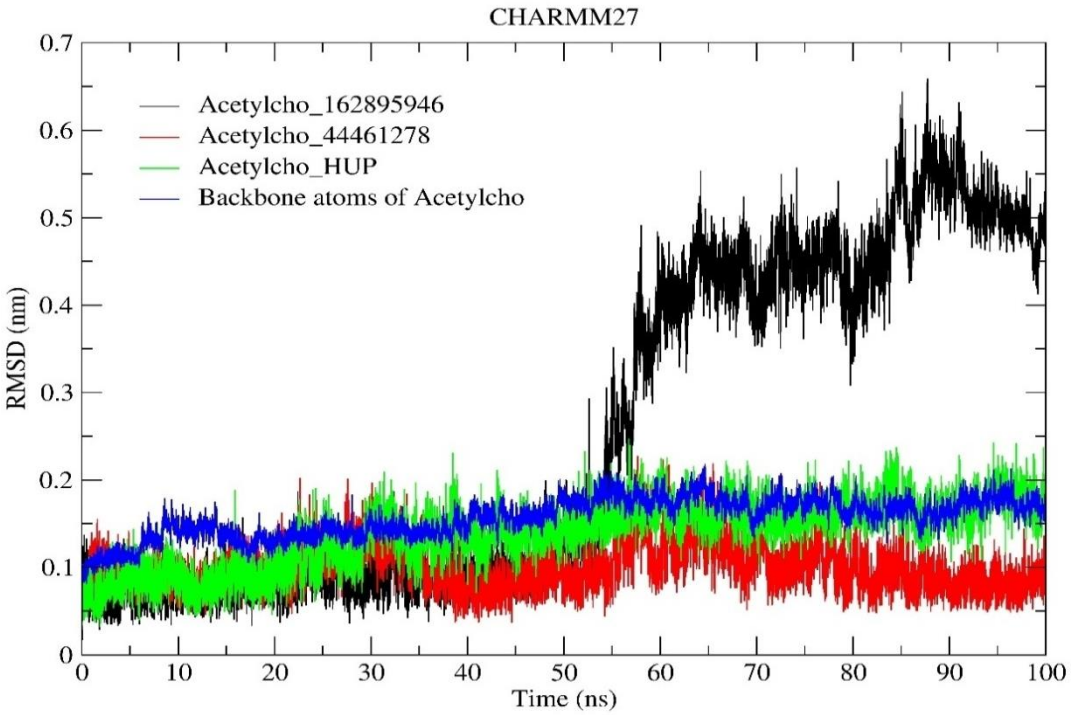

Figure .7. Root mean square deviation (RMSD) profiles for backbone atoms of each system.

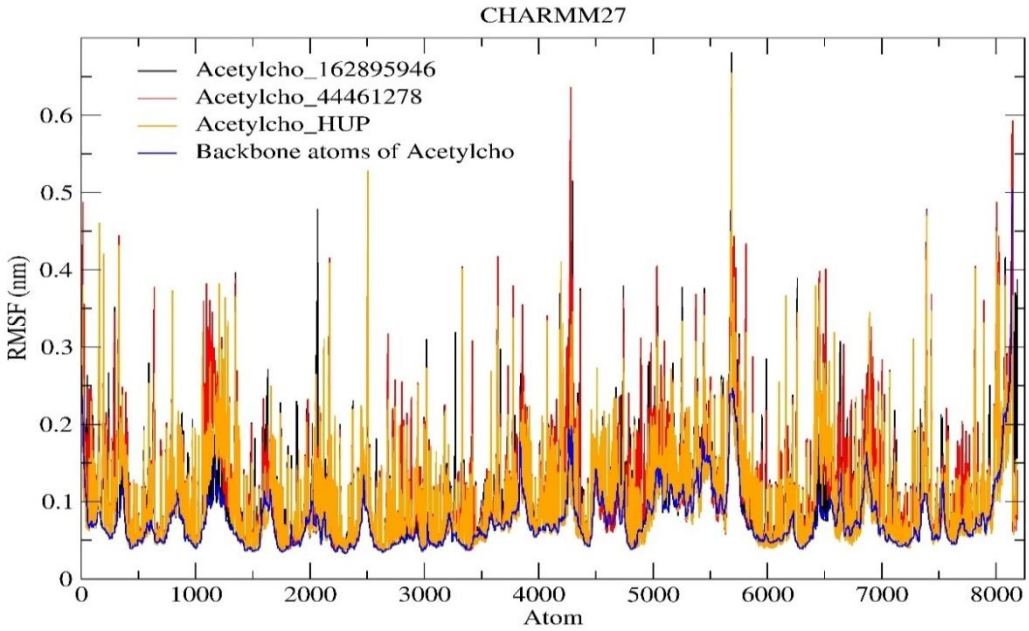

Figure .8. Root mean square Fluctuation (RMSF) profiles for backbone atoms of each system.

The root mean square fluctuation (RMSF) is a measure of the residual movement of amino acids. More specifically, high RMSF values imply high movement and flexibility in the active site. The extremely low RMSF values characterize a stable and inflexible active site. The RMSF profiles of the three complexes have been computed and are shown in **Figure 8**.The average values of each system were 0.115, 0.120, 0.110 and 0.075 nm for Acetylcholinesterase_162895946, Acetylcholinesterase_44461278, Acetylcholinesterase_HUP complexes and the backbone atoms of protein respectively.At this point, it is seen that, while binding with the hit compounds compared to the reference complex, the average RMSF values of the amino acid residues are almost identical overall.Every system's RMSF data showed some variations from their initial structures, indicating a dynamic shift. Additionally, all of the systems' fluctuation values matched those of Acetylcholinesterase alone, demonstrating the structural and biomolecular stability of the studied systems.Since the RMSF and RMSD analyses yielded similar results, it

appears that the proposed compounds may be promising candidates for the development of new and effective drugs for neurological diseases.

Radius of Gyration (Rg) Analysis

Radius of gyration (Rg)was estimated in this study to reflect the compactness of the three complexes.The calculated average Rg values for the Acetylcholinesterase_162895946, 44461278, and HUP complexes were 2.311, 2.315 and 2.309 nm respectively.There was no structural shifting in the Acetylcholinesterase configuration in the presence of the hit molecules, and it established a stable radius of gyration equilibrium, implying stability of the complexes during the 100 ns simulation.The calculated radius of gyration (Rg) of the three systems is shown in **Figure 9**.This high structural stability will encourage researchers studying neurodegenerative disorders to synthesize and test these compounds in vitro and in vivo.

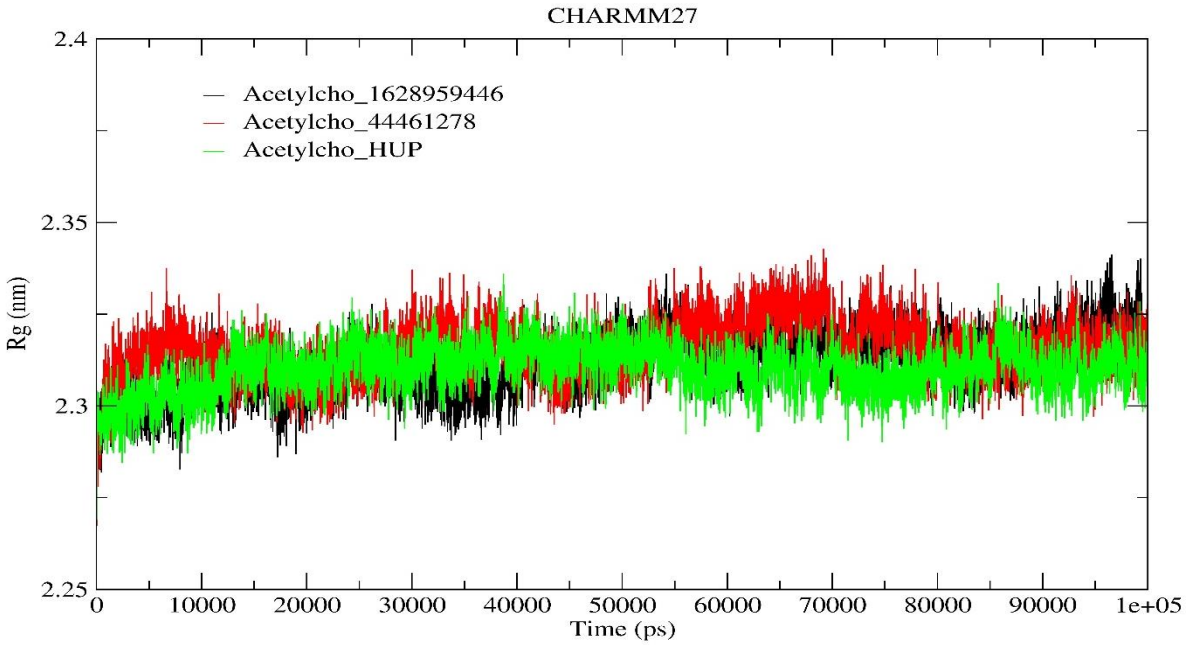

Figure .9. Radius of gyration (Rg) profiles for each system over 100 ns of simulation.

Solvent Accessible Surface Area (SASA) analysis

The solvent Accessible Surface Area forecasts the dynamical modifications seen throughout the interaction period. As shown in **Figure 10**, the average SASA value for the reference complex was 211.755 nm^2.While the average SASA values for both complexes (Acetylcholinesterase_162895946 and 44461278) were 212.665 and 216.149 nm^2 respectively (**Table 7**). The SASA achieved an equilibrium state without shifting across the simulation, indicating Acetylcholinesterase configurations stability in the presence of the two hit compounds.Ultimately, this commonality assists in clarifying the behavior of hit molecules with the active site of Acetylcholinesterase, as well as the formation of continuous binding during the molecular interactions.

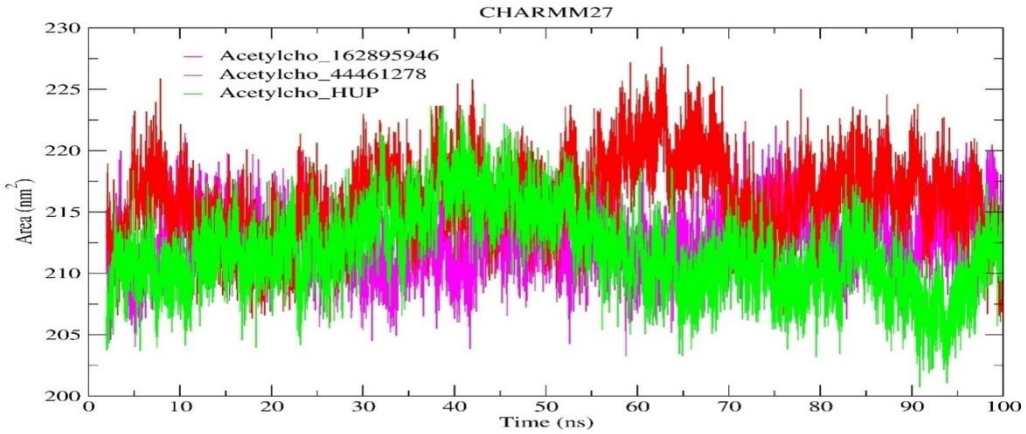

Figure 10. Solvent Accessible Surface Area (SASA) profiles for each system during 100 ns of simulation.

Table 7. The average values of different parameters obtained through MD simulation.

Parameters	**Acetylcholinesterase_ 162895946**	**Acetylcholinesterase_44461278**	**Acetylcholinesterase_ HUP**
RMSD (nm)	0.254	0.100	0.138
RMSF (nm)	0.115	0.120	0.110
Rg (nm)	2.311	2.315	2.309
SASA (nm^2)	212.665	216.149	211.755

4.7.Dynamic cross-correlation matrix (DCCM) analysis

The dynamic cross-correlation matrices examined the correlative movements of structural configurations to verify the stability of Acetylcholinesterase following interactions with the reference ligand (Huperzine is a clinical drug for Alzheimer disease.) and the two hit molecules from molecular dynamic data. The dynamic cross-correlation maps showed residual shifts inprotein. **Figure 11** depicts the positive and negative correlation of residue movement throughout the 100 ns of simulation.The color measure shows the degree of the correlation, with blue representing positive correlation ($^{+}1$) and red indicating negative correlation ($^{-}1$).A positive correlation reflects that the residues were moving in the identical orientation, whereas a negative

correlation confirms that the residues were moving in opposing orientations.On inspection of the dynamic cross-correlation matrix maps of the three systems, it was seen that the correlated motions exhibited by each system were quite comparable. The overall movements that demonstrate adirect correlation in the Acetylcholinesterase_162895946 complexstayed constant as compared to the Acetylcholinesterase_HUP complex, but the movements that indicate a negative correlation increased significantly, especially in the regions denoted by black boxes.Furthermore, at the atomic level, the hit molecule 44461278 formed a stablecomplex with the active site of Acetylcholinesterase.The results of the investigation align with the outcomes of molecular docking and measurementsobtained from dynamic simulation, confirming the efficacy of the selected compounds in inhibiting the biological functions of Acetylcholinesterase.

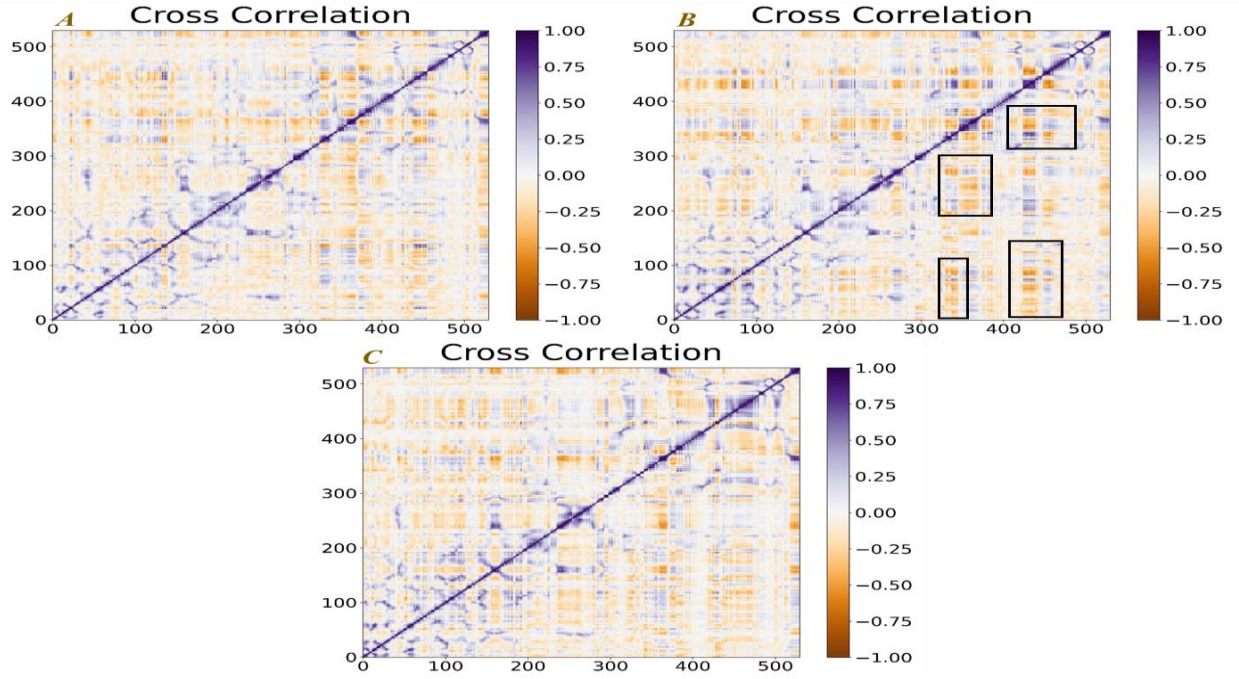

Figure 11.C_{α}residue cross-correlation computed for the three system, (**A**) 162895946, (**B**) 44461278 and (**C**) HUP.

4.8.Free energy landscape (FEL)

Demonstrating the nature of structural configurations that are dependent on the free energy landscape is crucial in determining the reason for protein aggregation [33]. To investigate the structural dynamics of Acetylcholinesterase after its biomolecular interactions with the three compounds, we developed a free energy landscape that represents protein configuration shifts. We selected two reaction parameters of the free energy landscape: the RMSD of Acetylcholinesterase (displaying protein structural stability during 100 ns of simulations) andthe radius of gyrate (representing the folding).**Figure 12** depicts the free energy landscape immediately following the interactions of Acetylcholinesterase with 162895946, 162895946 and HUP molecules.We found a major well located at (0.14 nm, 2.28 nm) when interacting with the hit molecule 162895946 and another key well located at (0.16 nm, 2.29 nm) when connecting with the hit molecule 44461278.However, upon interaction with a clinical Acetylcholinesterase inhibitor (HUP), we clearly observed a centered well at the coordinates (0.15 nm and 2.28 nm).Over the simulations, low-energy zones on the free-energy maps imply that the entire biomolecular structure and dynamics are reasonably stable.When the compound 44461278 was bound to the active site of Acetylcholinesterase, the large well from the FEL map confirmed again that this hit molecule forms a highly stable complex with the protein receptor when compared to the drug (HUP) currently used to treat Alzheimer and neurodegenerative diseases.Extraction of protein structures from the three areas revealed minor conformational changes in the protein structure after interacting with the two hit compounds. The results of FEL studies were particularly interesting since they were

able to differentiate the structures in terms of biomolecular structure and were similar to the results of RMSD, RMSF and DCCM analyses.

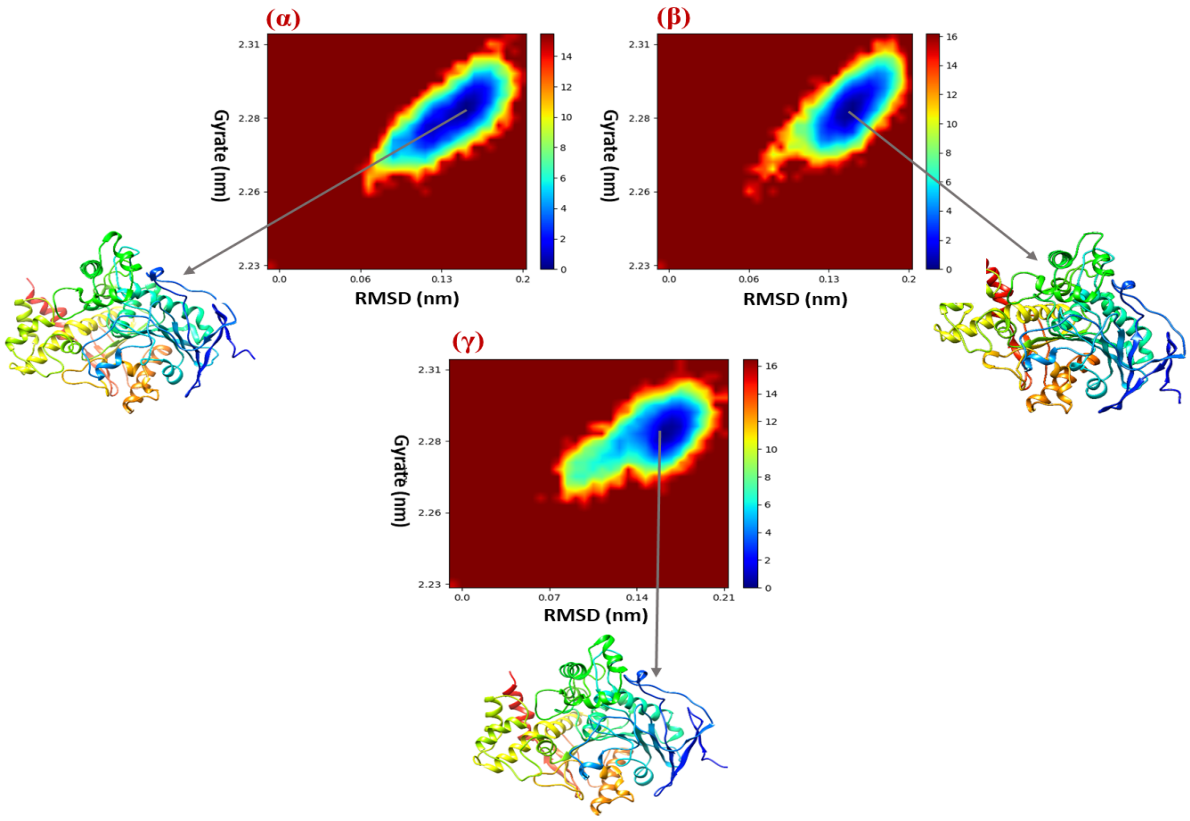

Figure .12.FEL as a function of RMSD (nm) and radius of gyration (nm) for (α)Acetylcholinesterase_162895946, (β)Acetylcholinesterase_44461278 and (γ)Acetylcholinesterase_HUP.Snapshots of Acetylcholinesterase structures from minimum energy basinswere extracted.

4.9.Binding Free Energy Calculations

MM-PBSA calculations were executed to conduct a comprehensive examination of the different binding energies that affect the interaction of the three ligands with the Acetylcholinesterase receptor. Non-covalent interactions are often prominent during interactions. Hydrophobic energies, hydrogen bonding, electrostatic interactionand Van der Waals energies are among the forces. Every one of these energiescontributes,

negatively or positively, to the total binding energy.The total binding free energy is comprised of several components, including van der Waals interactions (ΔE_{VDW}), electrostatic interactions (ΔE_{EEL}), polar component (ΔE_{GB}), non-polar contribution of attractive solute solvent interactions to the solvation energy (ΔE_{DISPER}),non-polar component of the solvation energy (ΔE_{SURF}), total gas phase molecular mechanics energy (ΔG_{GAS}), and total solvation energy (ΔG_{SOLV}).Electrostatic interactions were particularly prevalent in the binding of three complexes**(Table 8)**, with -281.00, -288.37, and -288.42 Kj/mol for Acetylcholinesterase_162895946, 44461278, and HUP complexes, respectively.Furthermore, as compared to the reference medication (HUP), the hit compound 44461278 forms a stable complex with the enzyme receptor.The findings of this investigation show that the hit molecules may have the ability to inhibit the biomolecular activity of this enzyme, and the molecular docking results were validated.

Table 8. The binding free energy in kcal.mol^{-1} for the three studied systems using MM-PBSA calculations.

	Acetylcholinesterase_162895946	**Acetylcholinesterase_44461278**	**Acetylcholinesterase_HUP**
ΔE_{VDW}	-38.67	-36.79	-35.42
ΔE_{EEL}	-281.00	-288.37	-288.42
ΔE_{GB}	286.30	288.64	290.01
ΔE_{SURF}	-4.48	-4.51	-4.31
ΔG_{GAS}	-319.66	-325.15	-323.85
ΔG_{SOLV}	281.82	284.13	285.70
Δ_{TOTAL}	-37.85	-41.02	-38.15

The binding energies of all residues are computed using MM-PBSA calculations and are shown in **Figure 13**.In addition, the common residues with a binding energy contribution in the three systems are Glu202, Trp86, Tyr119, Gly120, Gly121, Tyr124, Ser125, Glu202, Phe197 and Phe338. In Acetylcholinesterase_162895946

complex, the residues Trp86, Tyr124, Glu202 and Tyr337 contributed -6.95, -2.28, 3.19 and -1.95 kcal.mol^{-1} to the total binding

energy.While In Acetylcholinesterase_44461278 complex, the amino acid residues Trp86, Tyr119, Gly121, Glu202 and Tyr449 contributed -6.95, -2.28, 3.19 and -1,95 kcal.mol^{-1} to the total BE. In addition, in the reference complex with HUP molecules, the amino acid residues Trp86, Tyr119, Gly120, Gly121 and Tyr337 contributed -8.19, -1.08, -1.08, -1.4 and -3.17 kcal/mol to the total binding energy.All of this data suggests that interactions with amino acids (Trp86, Glu202, and Tyr237) is required to suppress the biochemical and cellular activities of Acetylcholinesterase, which might be importantin the development of potent treatment for Alzheimer and other neurodegenerative illnesses.

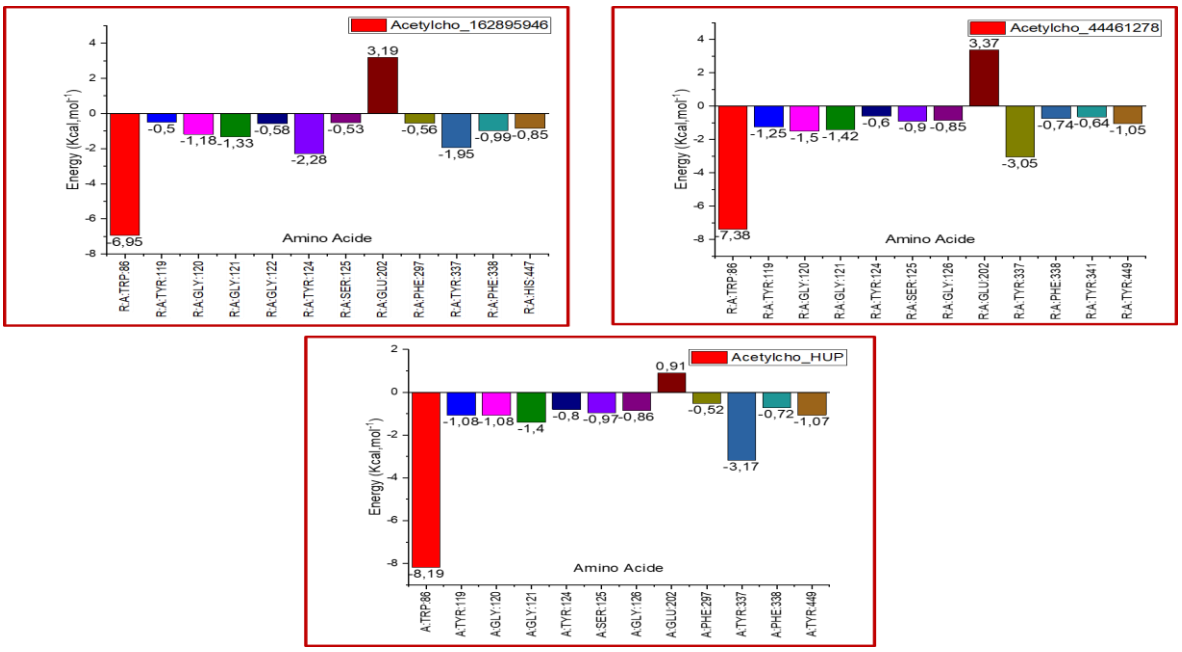

Figure .13.MM-PBSA binding energy decomposition for the three-exanimated systems.

References

1. Berman, H M.; Westbrook,J .; Feng,Z .; Gilliland,G.;Bhat, T N.; Weissig, H .;I Shindyalov, N.; Bourne, P E. The Protein Data Bank. NucleicAcidsResearch.

2. Sastry, G. M.;Adzhigirey, M.; Day, T.; Annabhimoju, R.; Sherman, W. Protein and Ligand Preparation: Parameters, Protocols, and Influence on Virtual Screening Enrichments. J Comput Aided Mol Des2013, 27 (3), 221–234. https://doi.org/10.1007/s10822-013-9644-8.

3. Čolović, M. B.;Krstić, D. Z.; Lazarević-Pašti, T. D.; Bondžić, A. M.; Vasić, V. M. AcetylcholinesteraseInhibitors: Pharmacology and Toxicology. CurrNeuropharmacol2013, 11 (3), 315–335. https://doi.org/10.2174/1570159X11311030006.

4. Chen, Y. L.; Nielsen, J.; Hedberg, K.; Dunaiskis, A.; Jones, S.; Russo, L.; Johnson, J.; Ives, J.; Liston, D. Syntheses, Resolution, and Structure-Activity Relationships of PotentAcetylcholinesteraseInhibitors: 8-Carbaphysostigmine Analogues. J Med Chem1992, 35 (8), 1429–1434. https://doi.org/10.1021/jm00086a011.

5. Chen, J.; Lai, L. Pocket v.2: FurtherDevelopments on Receptor-Based Pharmacophore Modeling. J. Chem. Inf. Model.2006, 46 (6), 2684–2691. https://doi.org/10.1021/ci600246s.

6. Son, M.; Park, C.; Rampogu, S.; Zeb, A.; Lee, K. Discovery of Novel AcetylcholinesteraseInhibitors as Potential Candidates for the Treatment of Alzheimer'sDisease. International Journal of Molecular Sciences 2019, 20, 1000. https://doi.org/10.3390/ijms20041000.

7. Michael, M. M.;Carchia, M.; Irwin, John. J.;Shoichet, B. K. Directory of UsefulDecoys, Enhanced (DUD-E): Better Ligands and Decoys for Better Benchmarking. J. Med. Chem.2012, 55 (14), 6582–6594. https://doi.org/10.1021/jm300687e.

8. Cheung,J. ; M, J. R. ; Fiana, B. ;Michael, S. C. ; Ebony ,N. G. ; James, L. ; Matthew,C. F. ; Jude, J. H.Structures of Human Acetylcholinesterase in ComplexwithPharmacologically Important Ligands | Journal of Medicinal Chemistry.https://pubs.acs.org/doi/10.1021/jm300871x.

9. Sahayarayan, J. J.;Rajan, K. S.; Vidhyavathi, R.; Nachiappan, M.; Prabhu, D.; Alfarraj, S.; Arokiyaraj, S.; Daniel, A. N. In-Silico Protein-Ligand Docking Studiesagainst the EstrogenProtein of Breast Cancer Using Pharmacophore Based Virtual Screening Approaches. Saudi Journal of Biological Sciences 2021, 28 (1), 400–407.https://doi.org/10.1016/j.sjbs.2020.10.023.

10. Anu, K. R. ; Sumit, R. B. ; Subham, D. ;Niraja, R. ;Shenoy,G.G. ; Varadaraj,B. ;Fayaz,S.M. ; Jayesh, M. ; Alex, J.E-Pharmacophore modelling, moleculardocking and dynamicsapproaches for in silico identification of acetylcholinesteraseinhibitorsfromnaturalproductsagainstAlzheimer'sdisease.https://doi.org/10.21203/rs.3.rs-3475912/v1.

11. Salam, N. K.;Nuti, R.; Sherman, W. Novel Method for Generating Structure-Based Pharmacophores UsingEnergeticAnalysis. J. Chem. Inf. Model.2009, 49 (10), 2356–2368. https://doi.org/10.1021/ci900212v.

12. Maryam, A.;Siddiqi, A.; Vedithi, S.; Ece, A.; Khalid, R. Identification of SelectiveInhibitors for Phosphodiesterase 5A Using E-Pharmacophore Modelling and Large-Scale Virtual Screening-Based Structure Guided Drug Discovery Approaches. Journal of Biomolecular Structure and. Dynamics 2023, 1–16. https://doi.org/10.1080/07391102.2023.2242491

13. Halgren, T. A.; Murphy, R. B.; Friesner, R. A.; Beard, H. S.; Frye, L. L.; Pollard, W. T.; Banks, J. L. Glide: A New Approach for Rapid, Accurate Docking and Scoring. 2. EnrichmentFactors in Database Screening. J Med Chem 2004, 47 (7), 1750–1759. https://doi.org/10.1021/jm030644s.

14. Loving, K.; Salam, N.; Sherman, W. EnergeticAnalysis of Fragment Docking and Application to Structure-Based Pharmacophore HypothesisGeneration. Journal of computer-aidedmolecular design 2009, 23, 541–554. https://doi.org/10.1007/s10822-009-9268-1.

15. Truchon, J.-F.;Bayly, C. Evaluating Virtual Screening Methods: Good and Bad Metrics for the "Early Recognition" Problem. Journal of chemical information and modeling 2007, 47, 488–508. https://doi.org/10.1021/ci600426e.

16. Friesner, R. A.; Banks, J. L.; Murphy, R. B.; Halgren, T. A.; Klicic, J. J.; Mainz, D. T.; Repasky, M. P.; Knoll, E. H.; Shelley, M.; Perry, J. K.; Shaw, D. E.; Francis, P.; Shenkin, P. S. Glide: A New Approach for Rapid, Accurate Docking and Scoring. 1. Method and Assessment of Docking Accuracy. J. Med. Chem.2004, 47 (7), 1739–1749. https://doi.org/10.1021/jm0306430.

17. Verdonk, M. L.; Cole, J. C.; Hartshorn, M. J.; Murray, C. W.; Taylor, R. D. ImprovedProtein–Ligand Docking Using GOLD. Proteins: Structure, Function, and Bioinformatics2003, 52 (4), 609–623. https://doi.org/10.1002/prot.10465.

18. Ioakimidis, L.;Thoukydidis, L.; Mirza, A.; Naeem, S.; Reynisson, J. Benchmarking the Reliability of QikProp. CorrelationbetweenExperimental and Predicted Values. QSAR &Combinatorial Science 2008, 27, 445–456. https://doi.org/10.1002/qsar.200730051.

19. Ouassaf M., Belaidi S., Khamouli S., Belaid H., Chtita S.(2021). Combined 3D-QSAR and molecular dockinganalysis of thienopyrimidinederivatives as staphylococcus aureus inhibitors. Acta ChimicaSlovenica. 68, 289–303.https://doi.org/10.17344/acsi.2020.5985

20. Zoete,V., Michel, A.C.;Aurélien,G.; Olivier, M.SwissParam: A fast force fieldgenerationtool for smallorganicmolecules. Journal of Computational Chemistry, 32(11), 2359–2368 | 10.1002/jcc.21816.https://doi: 10.1002/jcc.21816.

21. Spoel,D.V.D. ; Lindahl,E. ; Hess,B. ; Groenhof,G. ; E Mark,A. ; Berendsen,H.J.C. ; GROMACS: Fast, Flexible, and Free. Journal of computationalchemistry 2005, 26 (16). https://doi.org/10.1002/jcc.20291.

22. Bourougaa, L.;Ouassaf, M.; Shtaiwi, A. Discovery of Novel PotentDrugs for Influenza by Inhibiting the Vital Function of Neuraminidase via Fragment-Based Drug Design (FBDD) and Molecular Dynamics Simulation Strategies. Journal of Biomolecular Structure and Dynamics2023, 0 (0), 1–15. https://doi.org/10.1080/07391102.2023.2251065.

23. Anbarasu, K.;Jayanthi, S. Identification of CurcuminDerivatives as Human LMTK3Inhibitors for Breast Cancer: A Docking, Dynamics, and MM/PBSA Approach. 3 Biotech2018, 8 (5), 1–12. https://doi.org/10.1007/s13205-018-1239-6.

24. Bourougaa, L.;Mebarka, O.; Khan, S.; Htar, T. Pharmacophore-Based Virtual Screening, Molecular Docking and Molecular Dynamics Studies for the Discovery of Novel Neuraminidase Inhibitors. Journal of biomolecular structure &dynamics 2023, 1–13. https://doi.org/10.1080/07391102.2023.2225007.

25. Srinivasan, E.;Rajasekaran, R. Effect of β-Cyclodextrin-EGCG Complexion againstAggregated a-Synucleinthrough Density Functional Theory and DiscreteMolecular Dynamics. Chemical PhysicsLetters2019, 717, 38–46. https://doi.org/10.1016/j.cplett.2018.12.042.

26. McCammon, J. A. Protein Dynamics. Rep. Prog. Phys.1984, 47 (1), 1. https://doi.org/10.1088/0034-4885/47/1/001.

27. Papaleo, E.;Mereghetti, P.; Fantucci, P.; Grandori, R.; De Gioia, L. Free-Energy Landscape, Principal Component Analysis, and Structural Clustering to IdentifyRepresentative Conformations fromMolecular Dynamics Simulations: The Myoglobin Case. Journal of Molecular Graphics and Modelling2009, 27 (8), 889–899. https://doi.org/10.1016/j.jmgm.2009.01.006.

28. Homeyer, N.;Gohlke, H. Free Energy Calculations by the MolecularMechanics Poisson−Boltzmann Surface Area Method. MolecularInformatics 2012, 31 (2), 114–122https://doi.org/10.1002/minf.201100135.

29. Mitra, A.;Biswas, R.; Bagchi, A.; Ghosh, R. Insight into the Binding of a Synthetic Nitro-Flavone Derivativewith Human Poly (ADP-Ribose) Polymerase 1. International Journal of BiologicalMacromolecules 2019, 141, 444–459. https://doi.org/10.1016/j.ijbiomac.2019.08.242.

30. Ouassaf M., Belaidi S., Lotfy K., Daoud I., Belaidi H. (2018). Moleculardockingstudies and ADMET properties of new 1.2. 3 triazole derivatives for anti-breast cancer activity. Journal of Bionanoscience, 12, 26-36. https://doi.org/10.1166/jbns.2018.1505

31. Ouassaf, M.;Belaidi, S.; Chtita, S.; Lanez, T.; Abul Qais, F.; Md Amiruddin, H. CombinedMolecular Docking and Dynamics Simulations Studies of Natural Compounds as

PotentInhibitorsagainst SARS-CoV-2 Main Protease. Journal of Biomolecular Structure and Dynamics2022, 40 (21), 11264–11273. https://doi.org/10.1080/07391102.2021.1957712.

32. Ouassaf, M.;Bourougaa, L.; Al-Mijalli, S. H.; Abdallah, E. M.; Bhat, A. R.; A. Kawsar, S. M. Marine-Derived Compounds as PotentialInhibitors of Hsp90 for Anticancer and Antimicrobial Drug Development: A Comprehensive In Silico Study. Molecules 2023, 28 (24), 8074. https://doi.org/10.3390/molecules28248074.

33. Yang, L.-Q.; Ji, X.-L.; Liu, S.-Q. The Free Energy Landscape of ProteinFolding and Dynamics: A Global View. Journal of Biomolecular Structure and Dynamics2013, 31 (9), 982–992. https://doi.org/10.1080/07391102.2012.748536.

General conclusions

Many diseases have spread in recent years, and among these is Alzheimer's disease, which affects the most elite class of elders and is characterized as a neurological disease. It causes damage to nerve cells, causing several diseases such as lack of sleep, memory loss, and behavioral problems. The enzyme acetylcholinesterase is considered one of the most important enzymes that must be targeted for the treatment of Alzheimer's disease because it is the cause of the breakdown of the bonds of the neurotransmitter acetylcholine, which is responsible for the safety of nerve cells and ensuring their proper functioning. Therefore, the primary goal of this work will be to find new acetylcholinesterase inhibitors that have great therapeutic efficacy and few side effects. The computational method initially used for this study is that of the e-pharmacophore approach. This method is used to study the affinity between the database ligands and the protein (PDB code: 4EY5) in order to study to what extent the compound binds to the protein acetylcholinesterase, which is expressed by its Fitness Score value. Molecular docking is one of the most widely used approaches to study the affinity between newly designed compounds and the targeted enzyme and to better study the interaction between them. After launching the molecular docking calculation in XP mode], the result is filtered from the docking scores of the new AChE inhibitors studied, so the compounds are ranked as follows: CID_162895946, 44461278, 44285285, and 81108419 (-11.436, -11.107, -10.792, and -10.680 kcal/mol, respectively). All the score results found are higher than those of the Huperzine reference ligand (-10.217 kcal/mol). After an analysis of the molecular interactions, key amino acids are involved in hydrogen bond-type interactions with the chosen compounds within the AChE receptor during the metabolic phase, which can occur in order to release therapeutic activity. It is important to note that these two amino acids are the same ones involved in the active sites of AChE and Huperzine.

These results are in agreement with those found by Minky Son et al. This study provides information on the capacity of the ligands to bind at the active site of AChE and their potential for inhibition of its biological activity.

After the selection of compounds that have a high capacity to interact with the enzyme acytelcolineesterase, it is important to study their pharmacokinetic and toxic properties. Through the results of the ADMET study, it was found that all four compounds proposed have good intestinal absorption (easy and rapid) thanks to their small molecular weight. They also have good oral bioavailability and a high synthetic power. All molecules have the capacity to reach biological mommbranes (excellent distribution). At the level of hepatic metabolism, Huperzine and its four studied derivatives play the role of inhibiting hepatic enzymes such as those of the cytochrome p450 family. The high LogS value between -3.199 and -2.033 reflects the ease of renal elimination of the four selected hits. Thus, after these results, we can say that the compounds examined meet all the conditions for good pharmacokinetics and also for toxicity. All the compounds present a negative profile for hepatotoxicity, carcinogenicity, mutagenicity, and cytotoxicity with LD50 values greater than 500 mg/kg, which shows that they are not toxic. Molecular dynamics simulations were used to assess the stability of drugs that bind to protein receptors. The recommended marine compounds had average RMSD values that varied from 0.147 through 0.295 nm, with an average RMSF of 0.127 to 0.142 nm, indicating low atomic mobility and structural stability over 100 ns of simulation. Finally, molecular dynamics simulation, cross-dynamic correlation matrix, free energy landscape, and MM-PBSA calculations show that the two ligands CID_162895946 and CID_44461278 form extremely stable complexes with the enzyme acetylcholinesterase with a high binding affinity. As a

result, these two compounds are proposed for additional experimental studies as potential (AChE) inhibitors

Abstract:

Huperzine A (HUP) plays a crucial role in Alzheimer's therapy by enhancing cognitive function through increased cholinergic activity as a reversible acetylcholinesterase (AChE) inhibitor. Despite some limitations seen in AChE inhibitors, ongoing research remains dedicated to finding innovative and more effective treatments for Alzheimer's disease. To achieve the goal of the discovery of potential HUP analogues with improved physicochemical properties, less toxic properties, and high biological activity, many in silico methods were applied. Based on the acetylcholinesterase-ligand complex, an e-pharmacophore model was developed. Subsequently, a virtual screening involving a collection of 1762 natural compounds sourced from the PubChem database was performed. This screening yielded 131 compounds that exhibited compatibility with the established pharmacophoric hypothesis. These selected ligands were then subjected to molecular docking within the active site of the 4EY5 receptor. As a result, we identified four compounds that displayed remarkable docking scores and exhibited low free binding energy to the target. These top four compounds, CID_162895946, CID_44461278, CID_44285285, and CID_81108419, were submitted to ADMET prediction and molecular dynamic simulations, yielding encouraging findings in terms of pharmacokinetic characteristics and stability. Finally, molecular dynamics simulation, cross-dynamic correlation matrix, free energy landscape, and MM-PBSA calculations demonstrate that two ligands from the selected ligands form very resilient complexes with the enzyme acetylcholinesterase with significant binding affinity. Therefore, these two compounds are recommended for further experimental research as possible (AChE) inhibitors.

Keywords: Alzheimer, acetylcholinesterase,HUP, e-pharmacophore, docking, ADMET,moleculardynamics, MM-PBS

Abstrait:

L'huperzine A (HUP) joue un rôle crucial dans le traitement de la maladie d'Alzheimer en améliorant la fonction cognitive grâce à une activité cholinergique accrue en tant qu'inhibiteur réversible de l'acétylcholinestérase (AChE). Malgré certaines limites observées dans les inhibiteurs de l'AChE, les recherches en cours restent consacrées à la recherche de traitements innovants et plus efficaces pour la maladie d'Alzheimer. Pour atteindre l'objectif de découvrir des analogues potentiels de l'HUP présentant des propriétés physicochimiques améliorées, des propriétés moins toxiques et une activité biologique élevée, de nombreuses méthodes in silico ont été appliquées. Basé sur le complexe acétylcholinestérase-ligand, un modèle e-pharmacophore a été développé. Par la suite, un criblage virtuel impliquant une collection de 1 762 composés naturels provenant de la base de données PubChem a été réalisé. Cette sélection a donné 131 composés présentant une compatibilité avec l'hypothèse pharmacophorique établie. Ces ligands sélectionnés ont ensuite été soumis à un docking moléculaire au sein du site actif du récepteur 4EY5. En conséquence, nous avons identifié quatre composés présentant des scores d'amarrage remarquables et une faible énergie de liaison libre à la cible. Ces quatre principaux composés, CID_162895946, CID_44461278, CID_44285285 et CID_81108419, ont été soumis à des simulations de prédiction et de dynamique moléculaire ADMET, donnant des résultats encourageants en termes de caractéristiques pharmacocinétiques et de stabilité. Enfin, la simulation de dynamique moléculaire, la matrice de corrélation dynamique croisée, le paysage d'énergie libre et les calculs MM-PBSA démontrent que deux ligands des ligands sélectionnés forment des complexes très résilients avec l'enzyme acétylcholinestérase avec une affinité de liaison significative. Par conséquent, ces deux composés sont recommandés pour des recherches expérimentales plus approfondies en tant qu'inhibiteurs possibles (AChE).

Mots clés : Alzheimer, acétylcholinestérase, HUP, e-pharmacophore, docking, ADMET, dynamique moléculaire, MM-PBS